Zootaxa 2776: 13–48 (2011)
www.mapress.com/zootaxa/

Article

ISSN 1175-5326 (print edition)
ZOOTAXA
ISSN 1175-5334 (online edition)

Morphology and phylogenetic relationships of a remarkable new genus and two new species of Neotropical freshwater stingrays from the Amazon basin (Chondrichthyes: Potamotrygonidae)

MARCELO R. DE CARVALHO [1] & NATHAN R. LOVEJOY [2]

[1] *Departamento de Zoologia, Instituto de Biociências, Universidade de São Paulo, Rua do Matão, Trav. 14., no. 101, São Paulo, SP, CEP 05508-900, Brazil E-mail: mrcarvalho@ib.usp.br (corresponding author)*
[2] *Department of Biological Sciences, University of Toronto Scarborough, 1265 Military Trail, Toronto, ON, M1C 1A4, Canada E-mail: lovejoy@utsc.utoronto.ca*

Table of contents

Abstract

The morphology and phylogenetic relationships of a new genus and two new species of Neotropical freshwater stingrays, family Potamotrygonidae, are investigated and described in detail. The new genus, *Heliotrygon*, n. gen., and its two new species, *Heliotrygon gomesi*, n. sp. (type-species) and *Heliotrygon rosai*, n. sp., are compared to all genera and species of potamotrygonids, based on revisions in progress. Some of the derived features of *Heliotrygon* include its unique disc proportions (disc highly circular, convex anteriorly at snout region, its width and length very similar), extreme subdivision of suborbital canal (forming a complex honeycomb-like pattern anterolaterally on disc), stout and triangular pelvic girdle, extremely reduced caudal sting, basibranchial copula with very slender and acute anterior extension, and precerebral and frontoparietal fontanellae of about equal width, tapering very little posteriorly. Both new species can be distinguished by their unique color patterns: *Heliotrygon gomesi* is uniform gray to light tan or brownish dorsally, without distinct patterns, whereas *Heliotrygon rosai* is characterized by numerous white to creamy-white vermiculate markings over a light brown, tan or gray background color. Additional proportional characters that may further distinguish both species are also discussed. Morphological descriptions are provided for dermal denticles, ventral lateral-line canals, skeleton, and cranial, hyoid and mandibular muscles of *Heliotrygon*, which clearly corroborate it as the sister group of *Paratrygon*. Both genera share numerous derived features of the ventral lateral-line canals, neurocranium, scapulocoracoid, pectoral basals, clasper morphology, and specific patterns of the adductor mandibulae and spiracularis medialis muscles. *Potamotrygon* and *Plesiotrygon* are demonstrated to share derived characters of their ventral lateral-line canals, in addition to the presence of angular cartilages. Our morphological phylogeny is further corroborated by a molecular phylogenetic analysis of cytochrome *b* based on four sequences (637 base pairs in length), representing two distinct haplotypes for *Heliotrygon gomesi*. Parsimony analysis produced a single most parsimonious tree revealing *Heliotrygon* and *Paratrygon* as sister taxa (bootstrap proportion of 70%), which together are the sister group to a clade including *Plesiotrygon* and species of *Potamotrygon*. These unusual stingrays highlight that potamotrygonid diversity, both in terms of species composition and undetected morphological and molecular patterns, is still poorly known.

Key words: *Heliotrygon rosai*, *Heliotrygon gomesi*, taxonomy, systematics, Myliobatiformes, South America

Accepted by R. Pethiyagoda: 18 Feb. 2011; published: 24 Feb. 2011

Introduction

The Neotropical freshwater stingray family Potamotrygonidae has confounded researchers for many years in relation to its true diversity, proper species identification, and historical biology. Even though potamotrygonids have a long taxonomic history, dating to Alcide D. d'Orbigny's (1834) plate of *Trygon histrix* (Castex, 1963), confusion regarding basic taxonomic issues still abounds in the modern literature (e.g. Ross & Schäfer, 2000; Deynat, 2006; for a summary, see Carvalho et al., 2003). The family has been 'completely' taxonomically revised on at least three occasions, albeit with relatively large intervals of, coincidentally, 72 years (Müller & Henle, 1841; Garman, 1913; Rosa, 1985a). The last of these revisions, however, represented a significant advance in terms of species recognition and nominal species application.

Potamotrygonidae are the only living chondrichthyan supra-specific group that has diversified within a freshwater system (Thorson et al., 1983; Carvalho et al., 2003; Rosa et al., 2010). Their morphological distinctiveness was first recognized by Garman (1877), who placed them in their own group, the Potamotrygones. Subsequent to Garman's accounts (1877, 1913), and prior to Rosa's (1985a) taxonomic revision, the family was studied most notably by Mariano Castex, who described seven nominal species (sometimes with collaborators), of which only three appear to be valid (two for certain; Silva & Carvalho, in press). Carvalho et al. (2003), based on original work, summarized many aspects of potamotrygonid nomenclature, general biology and distribution, and were conservative in recognizing 18 species within the family, but noted that much of the species-level diversity was still awaiting formal description and that many older taxonomic issues remain unsolved (e.g. the validity of *Trygon garrapa* Jardine, 1843). Additional new species, based on material already present in collections, were recently described by Deynat (2006) and Rosa et al. (2008).

A more complete understanding of potamotrygonid intraspecific variation became possible only when significant collecting efforts were made by various researchers in different river systems within the Neotropical region. For example, potamotrygonids are more diverse in the Amazonian realm, but new species are also being described, after extensive analyses of large quantities of material, from the better-known Paraná-Paraguay system (Loboda & Carvalho, in prep.). Morphological and taxonomic revisions of many species and species-complexes, sometimes employing a basin-by-basin approach, are currently underway in the lab of the senior author; 13 new species of potamotrygonids are currently being described in the context of larger comparative morphological studies.

Material of the unusual new genus and species described below took some 10 years to assemble. The first specimen examined by one of us (MRC), in the early 1990s in the American Museum of Natural History, is a preadult male collected from the upper Amazon basin in 1988 (probably from Ecuador) and identified as *Paratrygon aiereba*. The second specimen was collected in 1993, but from much farther east in the mid-Purus basin in the Brazilian Amazon (also a preadult male, this time identified as *Plesiotrygon iwamae*). We subsequently received material made available through the aquarium trade, exported from Iquitos (Peru) and collected in the Rio Nanay, a tributary of the upper Rio Amazonas commonly known to harbor these 'round' or 'china' rays, as hobbyists have referred to them (Ross & Schäfer, 2000). We have now amassed, through collecting efforts of our own but especially through those of colleagues, 20 specimens which form the basis of the description below of a new potamotrygonid genus with two new species. Our material includes males and females, representing juvenile, pre-adult and adult specimens, and covers a very large geographic range, from near the mouth of the Amazon River to Peru and probably Ecuador. Our initial intentions were to collect specimens from more localities within this extended range in order to properly address intraspecific variation. But due to the difficulty of obtaining material from such a great range, it seems appropriate to describe both species in advance of more detailed morphological studies, which are presently in progress.

Material and Methods

Measurements taken on specimens were modified from Bigelow & Schroeder (1953), Hubbs & Ishiyama (1968) and Rosa (1985a). Measurements were transformed into percentages of disc width (% DW) to allow direct comparisons, and are briefly described as follows: **total length**, distance from tip of snout to tip of tail; **disc length**, greatest distance from tip of snout to posterior margin of disc; **disc width**, greatest distance between lateral margins of disc; **interorbital distance**, distance between upper margins of eyes; **interspiracular distance**, distance between

posterior margins of spiracles; **eye length**, greatest horizontal diameter of exposed portion of eyeball; **spiracle length**, oblique distance between anterior and posterior spiracular margins; **preorbital length**, distance from tip of snout to anterior margin of eyes; **prenasal length**, distance from tip of snout to anterior margin of nostrils; **preoral length**, distance from tip of snout to median portion of mouth slit; **internarial distance**, distance between anterior margins of nostrils; **mouth width**, greatest distance between lateral edges of mouth; **distance between 1st gill slits**, distance between inner margins of first pair of gill slits; **distance between 5th gill slits**, distance between inner margins of fifth pair of gill slits; **branchial basket length**, distance between outer margin of first and inner margin of fifth gill slits; **pelvic fin anterior margin length**, length of anterior margin of pelvic fin; **pelvic fin width**, greatest width between posterior margins of pelvic fins; **clasper external length**, distance from posterior margin of pelvic fin to tip of clasper; **clasper internal length**, distance from posterior margin of cloaca to tip of clasper; **distance between cloaca and tail tip**, distance from posterior margin of cloaca to tip of tail; **tail width**, greatest width of base of tail; **snout to cloaca distance**, distance from tip of snout to proximal margin of cloaca; **pectoral to posterior pelvic length**, distance from pectoral axil, at the joint of posterior margin of disc and tail, to posterior margin of pelvic fin; **distance from cloaca to sting origin**, distance from posterior margin of cloaca to base of first caudal sting; **sting length**, length of exposed portion of caudal sting; **sting width**, width taken at the origin of caudal sting.

Counts of fin rays and vertebrae mostly follow Compagno & Roberts (1982) and Rosa (1985a), excluding lower median teeth, mid-dorsal spines, and caudal vertebrae to base of sting, which were not recorded. Tooth rows were counted from radiographs and include all tooth rows, not just those exposed. Individual pectoral radial elements that are fused at their bases were counted separately, except for the anteriormost radial of the propterygium which was counted as a single element (in some specimens this is a compound element formed from two rays, but which diverges more distally, hence it was counted as a single element). Much fusion occurs at the bases of radials associated to all three pectoral basals, but counting them separately was uncontroversial. However, determination of the basal cartilage to which a radial fused at its base belongs is more difficult. This was addressed by associating a radial (fused at its base with other radials) to the basal occurring in a straight line from it. The mono- to diplospondyly transition occurred usually from between the first and fifth vertebral centrum caudal to the posterior margin of the pelvic girdle.

Skeletal structures were studied from dissected, radiographed, and cleared and stained individuals (prepared following Dingerkus & Uhler, 1977). The description of the skeleton is based on the entire skeleton in dorsoventral view. Adult claspers and cranial muscles are described for only one of the species, and lateral-line canals for the other, due to limitations of the material in hand. The morphological description is presented following the description of both new species. Photographs were taken with a digital camera, and illustrations were done employing a stereomicroscope equipped with a camera lucida attachment. X-ray radiographs were usually taken with Kodak mammography film (Min-R2000). Terminology for skeletal structures follows Nishida (1990) and Carvalho et al. (2004), for dermal denticles Deynat & Séret (1996), for muscles Miyake et al. (1988), for internal and external clasper components Taniuchi & Ishihara (1990), and for lateral-line canals Garman (1888), Ewart & Mitchell (1892), and Chu & Wen (1979). Anatomical abbreviations are provided in the figure legends.

Material examined of the new taxa is deposited in the following institutions: Academy of Natural Sciences of Philadelphia, Philadelphia (ANSP); American Museum of Natural History (AMNH); Cornell University (CU); and Museu de Zoologia da Universidade de São Paulo, São Paulo (MZUSP). Material was collected by several workers from the Rio Solimões (Brazil), lower Rio Amazonas (Pará state), and Rio Nanay, Peru. Seven additional specimens were acquired through the aquarium trade in Iquitos, Peru, which originated from the Rio Nanay, and from Ecuador (lacking more precise locality data). Comparative material examined of *Plesiotrygon* and *Paratrygon*, deposited in the MZUSP, is listed below (note that comparative material of *Potamotrygon*, amounting to some 1,400 specimens collected by the research groups of F. P. L. Marques and the first author, is too numerous to be separately listed). In addition, material listed in Carvalho et al. (2004) was also examined for the present study. Collected specimens were fixed *in loco* with injections of 10% formalin and subsequently transferred to 70% ethanol. Abbreviations used throughout the text include DL for disc length, DW for disc width, and TL for total length.

For the molecular phylogenetic analyses, muscle tissue from fresh material was excised and stored in 95% ethanol. Total genomic DNA was isolated from 1 mg of muscle tissue from four separate specimens of GENSP (ANSP 178014-178017) using DNeasy Tissue Kits (QIAGEN). The polymerase chain reaction (PCR) was used to amplify a ~700 base pair fragment of the mitochondrial cytochrome *b* gene using standard protocols. PCR products

were then purified using Montage PCR purification kit (Millipore) and sequenced using an ABI 377 Genetic Analyzer, using dye terminators (BigDye version 3.1, Applied Biosystems). Sequences were edited and aligned with previously published sequences from Lovejoy et al. (1998), available from Genbank. Parsimony analysis of the resultant matrix was conducted in PAUP* (Swofford, 2002) using the heuristic search algorithm with 1000 replicates of random addition of taxa, and TBR branch swapping. Bootstrap values were calculated in PAUP* using the heuristic search option (1000 replicates, 100 random taxon additions). Trees were rooted using *Himantura schmardae* and *H. pacifica* as outgroups.

Comparative material of *Plesiotrygon* and *Paratrygon* examined. *Paratrygon* (42 specimens): MZUSP 104402, Rio Tocantins, 11°15'48''S, 48°26'56''W, Ipueiras, Tocantins, Brazil, 18.vi.2005, coll. F. P. L. Marques, M. V. Domingues & G. Mattox (TO 05-33); MZUSP 104405, Rio Araguaia, 9°16'11''S, 49°58'18''W, Caseara, Tocantins, Brazil, 25.vi.2005, coll. F. P. L. Marques, M. V. Domingues & G. Mattox (TO 05-36); MZUSP 104406, Rio Araguaia, 9°16'11''S, 49°58'18''W, Caseara, Tocantins, Brazil, 25.vi.2005, coll. F. P. L. Marques, M. V. Domingues & G. Mattox (TO 05-37); MZUSP 104414, Rio Araguaia, 9°16'11''S, 49°58'18''W, Caseara, Tocantins, Brazil, 26.vi.2005, coll. F. P. L. Marques, M. V. Domingues & G. Mattox (TO 05-45); MZUSP 104029, Rio Tarauacá, 8°4'5''S, 70°43'4''W, Tarauacá, Acre, Brazil, 22.vii.2006, coll. F. P. L. Marques, N. M. Luchetti, V. M. Bueno & T. Loboda (AC 06-97); MZUSP 104646, Rio Urariquera, 3°22'51''S, 60°35'44''W, Boa Vista, Roraima, Brazil, 18.ii.2007, coll. F. P. L. Marques & M. R. Carvalho (AM 07-29); MZUSP 104647, Rio Urariquera, 3°22'51''S, 60°35'44''W, Boa Vista, Roraima, Brazil, 18.ii.2007, coll. F. P. L. Marques & M. R. Carvalho (AM 07-30); MZUSP 104648, Rio Urariquera, 3°22'51''S, 60°35'44''W, Boa Vista, Roraima, Brazil, 18.ii.2007, coll. F. P. L. Marques & M. R. Carvalho (AM 07-31), one specimen cleared & stained; MZUSP 104649, Rio Urariquera, 3°22'51''S, 60°35'44''W, Boa Vista, Roraima, Brazil, 18.ii.2007, coll. F. P. L. Marques & M. R. Carvalho (AM 07-32); MZUSP 104652, Rio Urariquera, 3°22'51''S, 60°35'44''W, Boa Vista, Roraima, Brazil, 18.ii.2007, coll. F. P. L. Marques & M. R. Carvalho (AM 07-35); MZUSP 104655, Rio Urariquera, 3°22'51''S, 60°35'44''W, Boa Vista, Roraima, Brazil, 20.ii.2007, coll. F. P. L. Marques & M. R. Carvalho (AM 07-38); MZUSP 104659, Rio Urariquera, 3°22'51''S, 60°35'44''W, Boa Vista, Roraima, Brazil, 21.ii.2007, coll. F. P. L. Marques & M. R. Carvalho (AM 07-42); MZUSP 104665, Rio Urariquera, 3°22'51''S, 60°35'44''W, Boa Vista, Roraima, Brazil, 24.ii.2007, coll. F. P. L. Marques & M. R. Carvalho (AM 07-48); MZUSP 104666, Rio Urariquera, 3°22'51''S, 60°35'44''W, Boa Vista, Roraima, Brazil, 24.ii.2007, coll. F. P. L. Marques & M. R. Carvalho (AM 07-49); MZUSP 104963, Rio Negro, 0°45'53''S, 62°56'35''W, Barcelos, Amazonas, Brazil, 24.ii.2004, coll. F. P. L. Marques & M. L. G. Araújo (RN 04-17); MZUSP 104965, Rio Negro, 0°58'38''S, 62°54'46''W, Barcelos, Amazonas, Brazil, 28.ii.2004, coll. F. P. L. Marques & M. L. G. Araújo (RN 04-50); MZUSP 104967, Rio Negro, 0° 58'38''S, 62°54'46''W, Barcelos, Amazonas, Brazil, 29.ii.2004, coll. F. P. L. Marques & M. L. G. Araújo (RN 04-58); MZUSP 104968, Rio Negro, 0° 58'38''S, 62°54'46''W, Barcelos, Amazonas, Brazil, 07.iii.2004, coll. F. P. L. Marques & M. L. G. Araújo (RN 04-95); MZUSP 104969, Rio Negro, 0° 58'38''S, 62°54'46''W, Barcelos, Amazonas, Brazil, 07.iii.2004, coll. F. P. L. Marques & M. L. G. Araújo (RN 04-96); MZUSP 104985, Rio Javari, 4°18'15''S, 70°4'19''W, Beijamin Constant, Amazonas, Brazil, 04.ix.2006, coll. M. V. Domingues & M. Cardoso Jr. (TA 06-14); MZUSP 104986, Rio Javari, 4°18'15''S, 70°4'19''W, Beijamin Constant, Amazonas, Brazil, 04.ix.2006, coll. M. V. Domingues & M. Cardoso Jr. (TA 06-15); MZUSP 104987, Rio Javari, 4°18'15''S, 70°4'19''W, Beijamin Constant, Amazonas, Brazil, 05.ix.2006, coll. M. V. Domingues & M. Cardoso Jr. (TA 06-16); MZUSP 103896, Rio Tapajós, 2°17'3''S, 55°0'13''W, Santarém, Pará, Brazil, 03.x.2005, coll. M. R. Carvalho, M. Cardoso Jr., M. L. G. Araújo & S. Mello (TJ05-02); MZUSP 103907, Rio Tapajós, 2°17'3''S, 55°0'13''W, Santarém, Pará, Brazil, 04.x.2005, coll. M. R. Carvalho, M. Cardoso Jr., M. L. G. Araújo & S. Mello (TJ05-14); MZUSP 103916, Rio Tapajós, 4°36'29''S, 56°16'22''W, Itaituba, Pará, Brazil, 09.x.2005, coll. M. R. Carvalho, M. Cardoso Jr., M. L. G. Araújo & S. Mello (TJ05-29); MZUSP 103917, Rio Tapajós, 4°36'29''S, 56°16'22''W, Itaituba, Pará, Brazil, 09.x.2005, coll. M. R. Carvalho, M. Cardoso Jr., M. L. G. Araújo & S. Mello (TJ05-30); MZUSP 104389, Rio Araguaia, 13°13'03''S, 50°35'07''W, São Miguel do Araguaia, Goiás, Brazil, 06.vi.2005, coll. F. P. L. Marques, M. V. Domingues & G. Mattox (TO 05-01); MZUSP 104390 (TO 05-02), same data as MZUSP 104389; MZUSP 104391, same data as MZUSP 104389 (TO 05-03); MZUSP 104392 (TO 05-04), same data as MZUSP 104389; MZUSP 104393 (TO 05-05), same data as MZUSP 104389; MZUSP 104394 (TO 05-06), same data as MZUSP 104389; MZUSP 104395 (TO 05-07), same data as MZUSP 104389; MZUSP 104396 (TO 05-08), same data as MZUSP 104389; MZUSP 104397 (TO 05-09), same data as MZUSP 104389; MZUSP 104398 (TO 05-10), same data as MZUSP

104389; MZUSP 104399 (TO 05-11), same data as MZUSP 104389; MZUSP 104400(TO 05-12), same data as MZUSP 104389; MZUSP 104401 (TO 05-13), same data as MZUSP 104389; MZUSP 104436, Rio Xingú, 6°39'23''S, 51°59'56''W, São Felix do Xingú, Pará, Brazil, 01.vii.2005, coll. F. P. L. Marques, M. V. Domingues & G. Mattox (TO 05-69); MZUSP 104444 (TO 05-79), same data as MZUSP 104436; MZUSP 104445 (TO 05-80), same data as MZUSP 104436.

Plesiotrygon (25 specimens): MZUSP 10153 (holotype), Rio Solimões, 3°22'S, 64°43'W, Tefé, Amazonas, Brazil, 03.x.1981, coll. H. Britski; FMNH 94500 (paratype), Rio Napo, Anangu, Napo, Ecuador, 10.x.1981, coll. D. Stewart, M. Ibarra & R. Barriga; MNRJ 573 (paratype), Rio Amazonas, Amazonas, Brazil, from Instituto Oswaldo Cruz; MZUSP 14789 (paratype), Rio Solimões, 3°25'S, 60°17'W, Amazonas, Brazil, i.1977, R/V Alpha Helix; USNM 258298 (paratype), Rio Solimões, Tabatinga, Amazonas, Brazil, 13.vi.1969, coll. T. B. Thorson et al.; ZMH 10343, Rio Solimões (paratype), Amazonas, Brazil, 6.xi.1909, coll. Scholz; MUSM 20328, Rio Pachitea, Puerto Inca, Peru. MZUSP 59896, Rio Solimões, 3°18'S, 67°92'W, Amazonas, Brazil, 22.xi.1993, coll. J. P. Friel et al.; MZUSP 59898, Rio Jutaí, 2°87'S, 66°93'W, Amazonas, Brazil, 16.xi.1993, coll. J. G. Lundberg et al.; MZUSP 59899, Rio Amazonas, 3°28'S, 58°57'W, Amazonas, Brazil, 20.x.1994, coll. Westneat et al.; MZUSP 42848, Baía de Marajó, Tupinambá, Pará, Brazil; MZUSP (uncat.), Baía de Marajó, 0°55'34''S, 48°17'25''W, Colares, Pará, Brazil, 16.viii.2007, coll. F. P. L. Marques, M. Cardoso Jr. & V. M. Bueno (PA 07-01); MZUSP (uncat.), Baía de Marajó, 0°55'34''S, 48°17'25''W, Colares, Pará, Brazil, 16.viii.2007, coll. F. P. L. Marques, M. Cardoso Jr. & V. M. Bueno (PA 07-08); MZUSP (uncat.), Baía de Marajó, 0°55'34''S, 48°17'25''W, Colares, Pará, Brazil, 20.viii.2007, coll. F. P. L. Marques, M. Cardoso Jr. & V. M. Bueno (PA 07-22); MZUSP (uncat.), Baía de Marajó, 0°55'34''S, 48°17'25''W, Colares, Pará, Brazil, 20.viii.2007, coll. F. P. L. Marques, M. Cardoso Jr. & V. M. Bueno (PA 07-23); MZUSP (uncat.), Baía de Marajó, 0°55'34''S, 48°17'25''W, Colares, Pará, Brazil, 20.viii.2007, coll. F. P. L. Marques, M. Cardoso Jr. & V. M. Bueno (PA 07-24); MZUSP (uncat.), Baía de Marajó, 0°55'34''S, 48°17'25''W, Colares, Pará, Brazil, 20.viii.2007, coll. F. P. L. Marques, M. Cardoso Jr. & V. M. Bueno (PA 07-27); MZUSP (uncat.), Baía de Marajó, 0°55'34''S, 48°17'25''W, Colares, Pará, Brazil, 20.viii.2007, coll. F. P. L. Marques, M. Cardoso Jr. & V. M. Bueno (PA 07-28); MZUSP (uncat.), Baía de Marajó, 0°55'34''S, 48°17'25''W, Colares, Pará, Brazil, 20.viii.2007, coll. F. P. L. Marques, M. Cardoso Jr. & V. M. Bueno (PA 07-29); MZUSP (uncat.), Baía de Marajó, 0°55'34''S, 48°17'25''W, Colares, Pará, Brazil, 20.viii.2007, coll. F. P. L. Marques, M. Cardoso Jr. & V. M. Bueno (PA 07-30); MZUSP (uncat.), Baía de Marajó, 0°55'34''S, 48°17'25''W, Colares, Pará, Brazil, 21.viii.2007, coll. F. P. L. Marques, M. Cardoso Jr. & V. M. Bueno (PA 07-38); MZUSP (uncat.), Baía de Marajó, 0°55'34''S, 48°17'25''W, Colares, Pará, Brazil, 22.viii.2007, coll. F. P. L. Marques, M. Cardoso Jr. & V. M. Bueno (PA 07-39); MZUSP (uncat.), Baía de Marajó, 0°55'34''S, 48°17'25''W, Colares, Pará, Brazil, 22.viii.2007, coll. F. P. L. Marques, M. Cardoso Jr. & V. M. Bueno (PA 07-40); MZUSP (uncat.), Baía de Marajó, 0°55'34''S, 48°17'25''W, Colares, Pará, Brazil, 22.viii.2007, coll. F. P. L. Marques, M. Cardoso Jr. & V. M. Bueno (PA 07-47); MZUSP (uncat.), Baía de Marajó, 0°55'34''S, 48°17'25''W, Colares, Pará, Brazil, 22.viii.2007, coll. F. P. L. Marques, M. Cardoso Jr. & V. M. Bueno (PA 07-48).

Family Potamotrygonidae Garman, 1913

Genus *Heliotrygon*, n. gen.

Diagnosis. *Heliotrygon* is distinguished from all other potamotrygonid genera by the following uniquely derived characters: disc very circular, without a median anterior concavity at snout (disc oval in *Paratrygon*, *Plesiotrygon* and *Potamotrygon* [slightly less so in *P. brachyura*], and with a clear anterior median concavity in *Paratrygon*); a highly reduced and barely noticeable caudal sting, shorter than spiracular length (sting usually at least as great as interorbital space in *Paratrygon*, *Plesiotrygon* and *Potamotrygon*), and devoid of acute lateral serrations (well-developed, sharp lateral serrations present in caudal stings of all three potamotrygonid genera); pelvic girdle very stout, with puboischiadic bar situated very obliquely in relation to median prepelvic process, resembling an upside-down "V" (puboischiadic process more perpendicular in *Plesiotrygon* and *Potamotrygon*, not nearly as stout in all three remaining genera of the family); lateral prepelvic process reduced to a broad lateral angle of the pelvic girdle (processes well-developed in *Potamotrygon* and *Plesiotrygon*, but slightly less developed in *Paratrygon*); anterior-most segment of propterygium closely contacts anterior margin of nasal capsule for half or most of its length (ante-

rior propterygial segment contacting nasal capsule only at its posteriormost point in *Paratrygon*, and contacts lateral, not anterior, margins of nasal capsules in *Potamotrygon* and *Plesiotrygon*); anterior propterygial segments almost contact each other medially (these farther apart in all three remaining potamotrygonid genera and widely distant in *Potamotrygon* and *Plesiotrygon*); metapterygium stout and highly arched, reaching laterally to level of propterygium (less stout and less arched in other potamotrygonid genera, not reaching laterally to level of propterygium); basibranchial copula with a very slender, acute anterior projection extending anteriorly to beyond level of ventral pseudohyoid bar (basibranchial anterior projection stouter in all three other potamotrygonid genera, triangular also in *Paratrygon* but more broadly so, not extending significantly beyond ventral pseudohyoid in *Potamotrygon* and *Plesiotrygon*).

Additional characters that distinguish *Heliotrygon* from other potamotrygonids, but not exclusive to *Heliotrygon* or of uncertain polarity within myliobatiforms, are as follows: nostrils circular, not slit-like (slit-like nostrils in *Potamotrygon* and *Plesiotrygon*); snout greatly elongated, preorbital length about one-third of disc width (snout much shorter, with preorbital length smaller than one-fourth disc width in *Potamotrygon* and *Plesiotrygon*); eyes very reduced in size, much smaller than spiracles (eyes about equal or smaller than spiracles in *Plesiotrygon* and *Potamotrygon*); spiracles without posterior knobs (present in *Paratrygon*); nostrils circular (elongated, slit-like in *Plesiotrygon* and *Potamotrygon*); branchial basket relatively short, about equal to internasal distance (branchial basket much greater than internasal space in *Plesiotrygon* and *Potamotrygon*); pelvic fins entirely concealed by posterior pectoral disc in dorsal view (pelvics protrude beyond disc in *Plesiotrygon* and *Potamotrygon*); tail width at base much less than one-half interorbital distance (roughly equal in *Plesiotrygon* and *Potamotrygon*); caudal sting situated relatively close to tail base (positioned farther posteriorly in *Potamotrygon* and *Plesiotrygon*); enlarged, acute spines over posterior disc midline and base of tail lacking (present in all three potamotrygonid genera in varying configurations); tail elongated and very slender, whip-like (tail stout and short in *Potamotrygon*, stout at base but slender distally in *Plesiotrygon*); lack of discrete angular cartilages (angulars present in *Plesiotrygon* and *Potamotrygon*); propterygium very wide and highly arched (clearly less wide and less arched in *Potamotrygon* and *Plesiotrygon*); scapulocoracoid very stout, wide and anteroposteriorly extended (these much more slender in *Plesiotrygon* and *Potamotrygon*); iliac processes reduced, not extending beyond level of ischial processes (projecting beyond level of ischial processes in *Potamotrygon* and *Plesiotrygon*); hyomandibulae relatively short, smaller than length of precerebral and frontoparietal fontenellae (greater in *Potamotrygon* and *Plesiotrygon*); nasal capsules separated by a relatively wide internasal septum (nasal capsules very close together with a very slender internasal septum in *Potamotrygon* and *Plesiotrygon*).

Type-species. *Heliotrygon gomesi*, n. sp., by original designation.

Included species. Currently the new genus is composed of two species, *Heliotrygon gomesi*, n. sp., and *Heliotrygon rosai*, n. sp., both described below.

Etymology. From the Greek *helios*, meaning "sun", in reference to its distinctively arranged pectoral disc radials that appear to "radiate" outward; and *trygon*, Greek for stingray. Gender feminine.

Remarks. The generic diagnosis above is based on characters that are common to both new species described below; monophyly of *Heliotrygon* is well supported. Even though the diagnosis is restricted to comparisons with other potamotrygonid genera, these same characters, either in isolation or in combination, serve to distinguish *Heliotrygon* from all other myliobatiform genera as well. *Urogymnus* Müller & Henle 1837, of uncertain validity (but cf. Last & Compagno, 1999; Compagno, 2005; Last & Stevens, 2009), also has a somewhat rounded disc, but much more oval and not nearly as circular as in *Heliotrygon*. The snout region in *Urogymnus* is also significantly shorter than in *Heliotrygon*. Furthermore, no other myliobatiform genus has a caudal sting as reduced as in *Heliotrygon*; although a few myliobatiform species lack caudal stings, these belong to genera in which the caudal stings are present as well developed structures in congeneric species. No nominal genus available for a potamotrygonid can be applied to our new species either. *Elipesurus* Schomburgk, 1843, following Rosa (1985a, b) and Carvalho et al. (2003) cannot be unequivocally applied and is best considered doubtful, whereas *Disceus* Garman, 1877 is a junior synonym of *Paratrygon* Duméril, 1865 (for further comments, see Rosa 1990; Carvalho et al., 2003). We note that the first authors to report on the distinctiveness of the new form were Ishihara & Taniuchi (1995), based on a juvenile aquarium specimen reportedly from the Orinoco basin (locality unconfirmed).

Most specimens of both new species do not have caudal stings, but these may be damaged upon being captured, and appear not to be as firmly attached as in other potamotrygonids or myliobatiforms. Under magnification, however, a small groove on the dorsal tail base is clearly visible where the caudal sting was originally located, even

in smaller specimens. The lack of caudal stings in some specimens therefore does not invalidate this feature (i.e. reduced caudal sting) as a generic-level diagnostic character, one considered (see below) to be derived in *Heliotrygon*.

Both species of *Heliotrygon* have greatly reduced eyes and are sometimes captured in relatively deeper channels of usually murky rivers in the Amazon basin. In this regard, species of this genus have a life-style and geographic distribution that is notably similar to *Plesiotrygon iwamae*, and we expect that specimens of *Heliotrygon* spp. will be captured where *Plesiotrygon iwamae* is known to occur. Parallels with other batoid genera are present in the morphology of *Heliotrygon* as well. Species of *Heliotrygon* and *Gymnura* (and also *Paratrygon*) are relatively flat and wide batoids that have expanded scapulocoracoids, pectoral basals and pectoral radials, morphological designs that provide enhanced skeletal support for the disc region. However, these similarities are clearly independently derived for *Gymnura* and *Heliotrygon* + *Paratrygon* (see Phylogenetic relationships of *Heliotrygon*, below).

At present, only two new species are described in *Heliotrygon*, but more material from a greater distribution is needed in order to shed light on morphological variation within and among species. Individuals of both species present variation in coloration that requires further study.

***Heliotrygon gomesi*, n. sp.**
Figures 1–9; Tables 1–2

Holotype. MZUSP 104988, adult female, Rio Jamari, 04°18'15"S, 070°04'19"W, Benjamin Constant, Amazonas, Brazil, 05.ix.2006, coll. M. C. Júnior & M. V. Domingues (TA 06–17). (Figures 1, 8, 9B).

Paratypes. (6 specimens). AMNH 251884, adult female, Rio Nanay, Rio Amazonas, Iquitos, Loreto, Peru (aquarium trade); ANSP 178014, adult male, Rio Nanay, Rio Amazonas basin, upstream from Pampa Chica, village 4.5 km west of Iquitos, Maynas, Loreto, Peru, coll. Linder Isuiza & ornamental fishermen, August 1999 to August 2001; ANSP 178015, adult (?) female, same data as ANSP 178014; ANSP 178016, adult male, same data as ANSP 178014; ANSP 178017, preadult (?) female, same data as ANSP 178014; MZUSP 108203, preadult female, Rio Nanay, Rio Amazonas basin, Iquitos, Loreto, Peru, coll. F. Marques (PU 09-33), 19.x.2009.

Other material. (6 specimens). AMNH 58402, preadult male, aquarium trade specimen reportedly from Ecuador (CJF, 24.xi.1988); AMNH (uncat.), preadult male (BES 04-00), Iquitos, Loreto, Peru (aquarium trade, probably from Rio Nanay, Rio Amazonas basin); AMNH (uncat.), preadult male, Iquitos, Loreto, Peru (aquarium trade, probably from Rio Nanay, Rio Amazonas basin); CU 78485, preadult (?) female, Iquitos, Loreto, Peru (aquarium trade, probably from Rio Nanay, Rio Amazonas basin); CU 78486, preadult (?) female, Iquitos, Loreto, Peru (aquarium trade, probably from Rio Nanay, Rio Amazonas basin); MZUSP 108294, aborted late-term pup from holotype, female, 125 mm DW, 135 mm DL, same data as holotype (specimen is cleared and stained).

Diagnosis. A species of *Heliotrygon* diagnosed by its unique dorsal color pattern, composed of a uniform gray to light tan or brown color, without strong vermiculations, rosettes or other conspicuous patterns dorsally. *Heliotrygon gomesi* is tentatively further separated from *H. rosai* (described below) by presenting a slightly more slender tail width at base (holotype tail width 4.5% DW *vs*. 5.6% DW in holotype of *H. rosai*), slightly greater preorbital snout length (holotype preorbital snout length 33.2% DW *vs*. 31.0% DW in holotype of *H. rosai*), and proportionally smaller pelvic inner length (2.1% DW in holotype of *H. gomesi*, and ranging from 1.0 to 3.3% DW in all specimens, with a mean of 1.9% DW *vs*. 4.6% DW in holotype of *H. rosai*, ranging from 1.3 to 4.9% DW in all specimens, with a mean of 3.7% DW).

Description. Measurements, as both raw data in mm and transformed into %DW, are presented in Table 1; meristic data are given in Table 2. The description below is based on all specimens, but salient features of the holotype are separately mentioned. For the description below, refer to Figures 1–9.

External morphology. Disc very flat, its greatest height more or less equal to, or slightly greater than, interorbital space. Disc very circular, widest more or less at its midlength. Disc slightly longer than wide in all specimens; disc length varying from 102.2 to 108.0% DW (x = 104.7% DW; disc proportionally longest in holotype). Snout very broad, elongated, convex. Preorbital snout length about four times interorbital distance, ranging from 32.6 to 35.7% DW (x = 34.2% DW; 33.2% DW in holotype). Prenasal (26.7 to 31.2% DW, x = 29% DW, holotype 28.4% DW) and preoral (29.5 to 35.7% DW, x = 32.5% DW, holotype 32.2% DW) snout lengths also proportionally elon-

gate. Snout with strongly circular anterior margin, and with minute rostral knob protruding from anterior disc (more prominent in smaller specimens). Posterior disc region slightly more oval than anterior disc region.

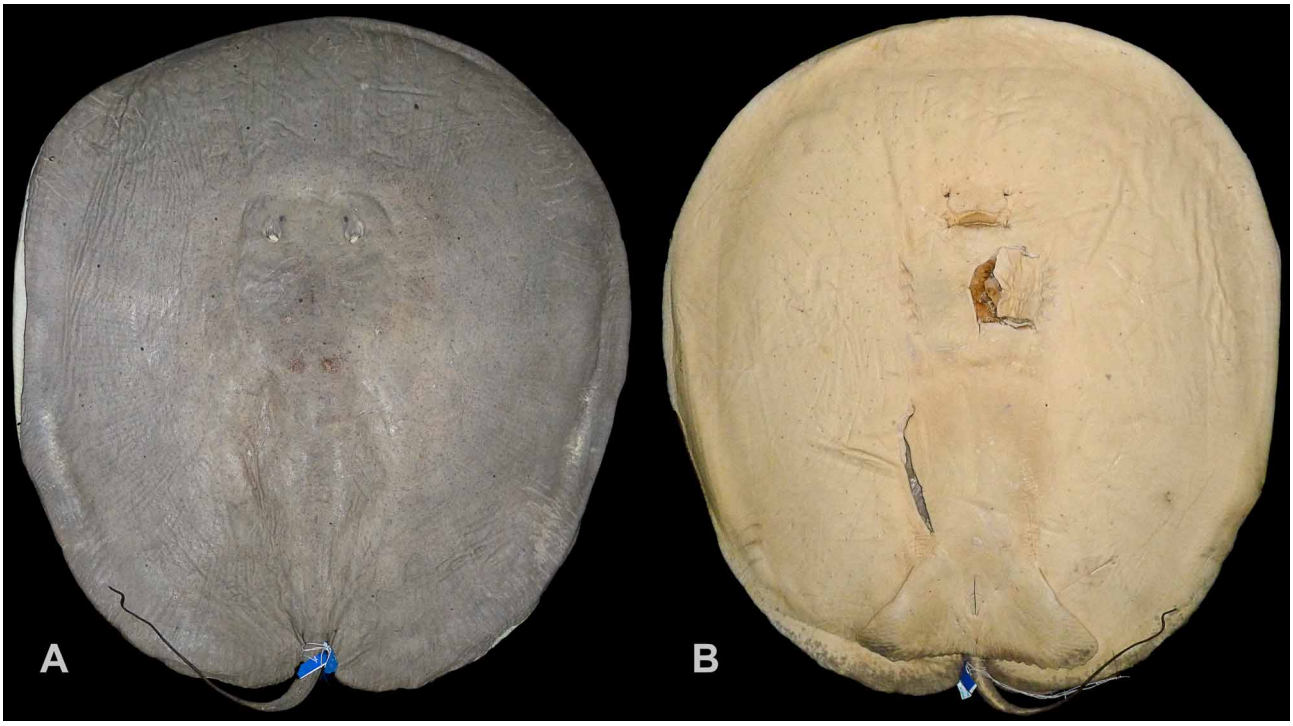

FIGURE 1. Holotype of *Heliotrygon gomesi*, n. sp., in dorsal (A) and ventral (B) views (MZUSP 104988, adult female, Rio Jamari, Amazonas state, Brazil; 836 mm TL, 624 mm DL, and 578 mm DW). Ventral dissections were made to remove parasites and for DNA extraction.

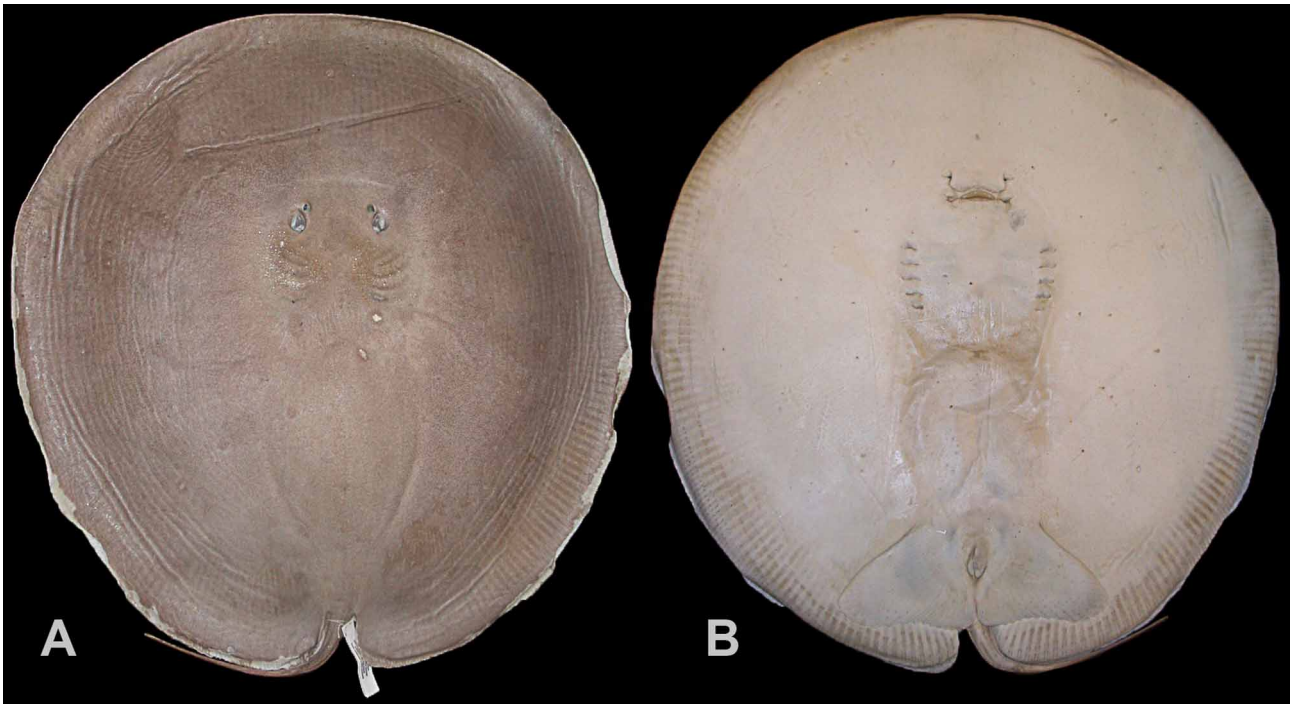

FIGURE 2. Paratype of *Heliotrygon gomesi*, n. sp., in dorsal (A) and ventral (B) views (AMNH 251884, adult female, Rio Nanay, Rio Amazonas, Iquitos, Peru; 684 mm TL, 557 mm DL, and 537 mm DW).

TABLE 1. Measurements of specimens of *Heliotrygon gomesi*, n. sp. A: MZUSP 104988 (holotype), adult female. B: AMNH 251884 (paratype), adult female. C: MZUSP 108203 (paratype), juvenile female. D: ANSP 178014 (paratype) adult male. E: ANSP 178015 (paratype), adult (?) female. F: ANSP 178016 (paratype), adult male. G: ANSP 178017 (paratype), juvenile female. H: AMNH 58402, preadult male. I: AMNH (uncat.), preadult male. *x*: mean. SD: standard deviation.

PARAMETER	A		B		C		D		E		F		G		H		I	
	mm	% DW	mm	% DW	mm	% DW	mm	% DW	mm	% DW	mm	% DW	mm	% DW	mm	% DW	mm	% DW
total length (TL)	836.0	-	684.0	-	494.0	-	520.0	-	785.0	-	480.0	-	425.0	-	422.0	-	772.0	-
disc length (DL)	624.0	108.0	557.0	103.7	290.0	107.8	420.0	105.0	410.0	104.3	465.0	105.7	230.0	102.7	361.0	104.6	327.0	102.2
disc width (DW)	578.0	100.0	537.0	100.0	269.0	100.0	400.0	100.0	393.0	100.0	440.0	100.0	224.0	100.0	345.0	100.0	320.0	100.0
interorbital distance	57.0	9.9	56.0	10.4	27.0	10.0	36.0	9.0	35.0	8.9	40.0	9.1	23.0	10.3	37.0	10.7	36.0	11.3
interspiracular distance	59.0	10.2	62.0	11.5	34.0	12.6	41.0	10.3	39.0	9.9	45.0	10.2	28.0	12.5	44.0	12.8	43.0	13.4
eye length	4.0	0.7	7.0	1.3	4.0	1.5	5.0	1.3	6.0	1.5	7.0	1.6	4.5	2.0	6.0	1.7	5.0	1.6
spiracle length	25.0	4.3	28.0	5.2	10.0	3.7	15.0	3.8	12.0	3.1	15.0	3.4	9.0	4.0	22.0	6.4	21.0	6.6
preorbital length	192.0	33.2	175.0	32.6	96.0	35.7	135.0	33.8	134.0	34.1	156.0	35.5	73.0	32.6	120.0	34.8	111.0	34.7
prenasal length	164.0	28.4	157.0	29.2	84.0	31.2	107.0	26.8	109.0	27.7	123.0	28.0	64.0	28.6	104.0	30.1	94.0	29.4
preoral length	186.0	32.2	179.0	33.3	96.0	35.7	118.0	29.5	122.0	31.0	130.0	29.5	71.0	31.7	117.0	33.9	108.0	33.8
internarial distance	48.0	8.3	51.0	9.5	25.0	9.3	35.0	8.8	32.0	8.1	39.0	8.9	21.0	9.4	38.0	11.0	36.0	11.3
mouth width	58.0	10.0	60.0	11.2	27.0	10.0	46.0	11.5	42.0	10.7	45.0	10.2	28.0	12.5	41.0	11.9	40.0	12.5
distance between 1st gill slits	116.0	20.1	107.0	19.9	51.0	19.0	77.0	19.3	75.0	19.1	85.0	19.3	47.0	21.0	73.0	21.2	66.0	20.6
distance between 5th gill slits	98.0	17.0	99.0	18.4	47.0	17.5	68.0	17.0	64.0	16.3	77.0	17.5	38.0	17.0	66.0	19.1	58.0	18.1
branchial basket length	62.0	10.7	51.0	9.5	29.0	10.8	39.0	9.8	40.0	10.2	45.0	10.2	26.0	11.6	36.0	10.4	36.0	11.3
pelvic fin anterior margin length	104.0	18.0	94.0	17.5	46.0	17.1	60.0	15.0	62.0	15.8	80.0	18.2	44.0	19.6	69.0	20.0	61.0	19.1
pelvic fins width	219.0	37.9	216.0	40.2	112.0	41.6	107.0	26.8	160.0	40.7	165.0	37.5	76.0	33.9	150.0	43.5	145.0	45.3
clasper external length	-	-	-	-	-	-	63.0	15.8	-	-	74.0	16.8	-	-	7.0	2.0	8.0	2.5
clasper internal length	-	-	-	-	-	-	62.0	15.5	-	-	65.0	14.8	-	-	37.0	10.7	37.0	11.6
distance between cloaca and tail tip	310.0	53.6	223.0	41.5	240.0	89.2	195.0	48.8	429.0	109.2	100.0	22.7	214.0	95.5	128.0	37.1	514.0	160.6
tail width	26.0	4.5	35.0	6.5	12.0	4.5	22.0	5.5	18.0	4.6	17.0	3.9	12.0	5.4	24.0	7.0	25.0	7.8
snout to cloaca distance	510.0	88.2	446.0	83.1	240.0	89.2	322.0	80.5	325.0	82.7	358.0	81.4	192.0	85.7	287.0	83.2	257.0	80.3
pectoral to posterior pelvic length	12.0	2.1	6.0	1.1	9.0	3.3	-	-	-	-	-	-	4.0	1.8	-	-	-	-
distance from cloaca to sting origin	111.0	19.2	94.0	17.5	-	-	76.0	19.0	-	-	80.0	18.2	-	-	73.0	21.2	-	-
sting length	13.0	2.2	7.0	1.3	-	-	12.0	3.0	-	-	5.0	1.1	-	-	11.0	3.2	-	-
sting width	1.0	0.2	1.0	0.2	-	-	1.5	0.4	-	-	1.0	0.2	-	-	1.8	0.5	-	-

TABLE 1 (cont.). Measurements of specimens of *Heliotrygon gomesi*, n. sp. J: CU 78485, preadult female. K: CU 78486, preadult female. L: AMNH (uncat.), preadult male. *x*: mean. SD: standard deviation.

PARAMETER	J		K		L		RANGE	*x*		SD	
	mm	% DW	mm	% DW	mm	% DW	% DW	mm	% DW	mm	% DW
total length (TL)	366.0	-	665.0	-	435.0	-	-	573.7	-	164.8	-
disc length (DL)	320.0	104.9	338.0	104.0	354.0	102.9	102.2–108.0	391.3	104.7	112.4	1.8
disc width (DW)	305.0	100.0	325.0	100.0	344.0	100.0	-	373.3	-	104.0	-
interorbital distance	32.0	10.5	38.0	11.7	39.0	11.3	8.9 –11.7	38.0	10.3	10.0	0.9
interspiracular distance	31.0	10.2	43.0	13.2	45.0	13.1	9.2–14.3	42.8	11.7	10.0	1.4
eye length	5.0	1.6	5.0	1.5	5.0	1.5	0.7–2.0	5.3	1.5	1.0	0.3
spiracle length	10.0	3.3	21.0	6.5	24.0	7.0	3.0–7.0	17.7	4.8	6.6	1.5
preorbital length	104.0	34.1	116.0	35.7	121.0	35.2	32.6–35.7	127.8	34.3	33.5	1.1
prenasal length	85.0	27.9	98.0	30.2	105.0	30.5	26.7–31.2	107.8	29.0	28.8	1.3
preoral length	95.0	31.1	113.0	34.8	117.0	34.0	29.5–35.7	121.0	32.5	32.7	2.0
internarial distance	25.0	8.2	36.0	11.1	38.0	11.0	8.1–11.2	35.3	9.6	8.9	1.2
mouth width	34.0	11.1	41.0	12.6	44.0	12.8	9.5–12.8	42.2	11.4	10.0	1.0
distance between 1st gill slits	61.0	20.0	70.0	21.5	70.0	20.3	19.0–21.5	74.8	20.1	20.2	0.9
distance between 5th gill slits	52.0	17.0	61.0	18.8	65.0	18.9	16.3–19.1	66.1	17.7	18.3	0.9
branchial basket length	33.0	10.8	39.0	12.0	38.0	11.0	8.2–12.0	39.5	10.7	9.7	0.7
pelvic fin anterior margin length	56.0	18.4	62.0	19.1	63.0	18.3	15.0–20.0	66.8	18.0	17.9	1.5
pelvic fin width	110.0	36.1	153.0	47.1	139.0	40.4	26.7–47.1	146.0	39.2	42.4	5.4
clasper external length	-	-	-	-	8.0	2.3	2.0–16.8	32.0	7.9	33.5	7.7
clasper internal length	-	-	-	-	42.0	12.2	8.7–15.5	48.6	13.0	13.8	2.1
distance between cloaca and tail tip	90.0	29.5	387.0	119.1	148.0	43.0	22.7–202.6	248.2	70.8	135.7	43.0
tail width	12.0	3.9	13.0	4.0	25.0	7.3	3.9–7.8	20.1	5.4	7.3	1.4
snout to cloaca distance	265.0	86.9	278.0	85.5	288.0	83.7	80.5–89.2	314.0	84.2	88.8	2.9
pectoral to posterior pelvic length	3.0	1.0	-	-	-	-	1.0–3.3	6.8	1.9	3.7	0.9
distance from cloaca to sting origin	-	-	-	-	-	-	17.5–21.2	86.8	19.0	15.7	1.4
sting length	-	-	-	-	-	-	1.1–3.2	9.6	2.2	3.4	0.9
sting width	-	-	-	-	-	-	0.2–0.5	1.3	0.3	0.4	0.1

Eyes minute, smaller than spiracles, and not greatly protruding above disc. Spiracles closely adjacent to eyes, rhomboidal in shape; spiracles about as wide as long, without elevated spiracular rims or central knob posteriorly. Mouth opening relatively straight across, its width about one-half distance between first gill slits, and more or less equal to internarial distance. Posterior profile of lower jaw marked with rugose grooves, but labial folds absent; outer corners of mouth also with marked grooves. Nostrils slightly smaller than eye-diameter, relatively circular. Nasal curtain medially notched at posterior margin; posterior margin highly fringed. Lateral margins of nasal curtain reaching to midlength of nostrils. Teeth externally visible with mouth closed; tooth row counts from radiographs 21–29/21–32; 29/28 exposed rows in holotype. Adult males with sharp, pointed cusps; adult females with smaller, less pointed and more broadly triangular cusps. Shallow integumental rugae posterior to mouth and anterior to gill-basket region. Branchial basket relatively short anteroposteriorly, much shorter than wide (branchial basket about half as long as wide; in holotype distance between first gill slits is 20.1% DW, and branchial basket length is 10.7% DW). Distance between first gill slits slightly greater than distance between fifth gill slits. Gill openings with slightly undulated gill flap; fifth gill slit smallest, slightly more obliquely positioned.

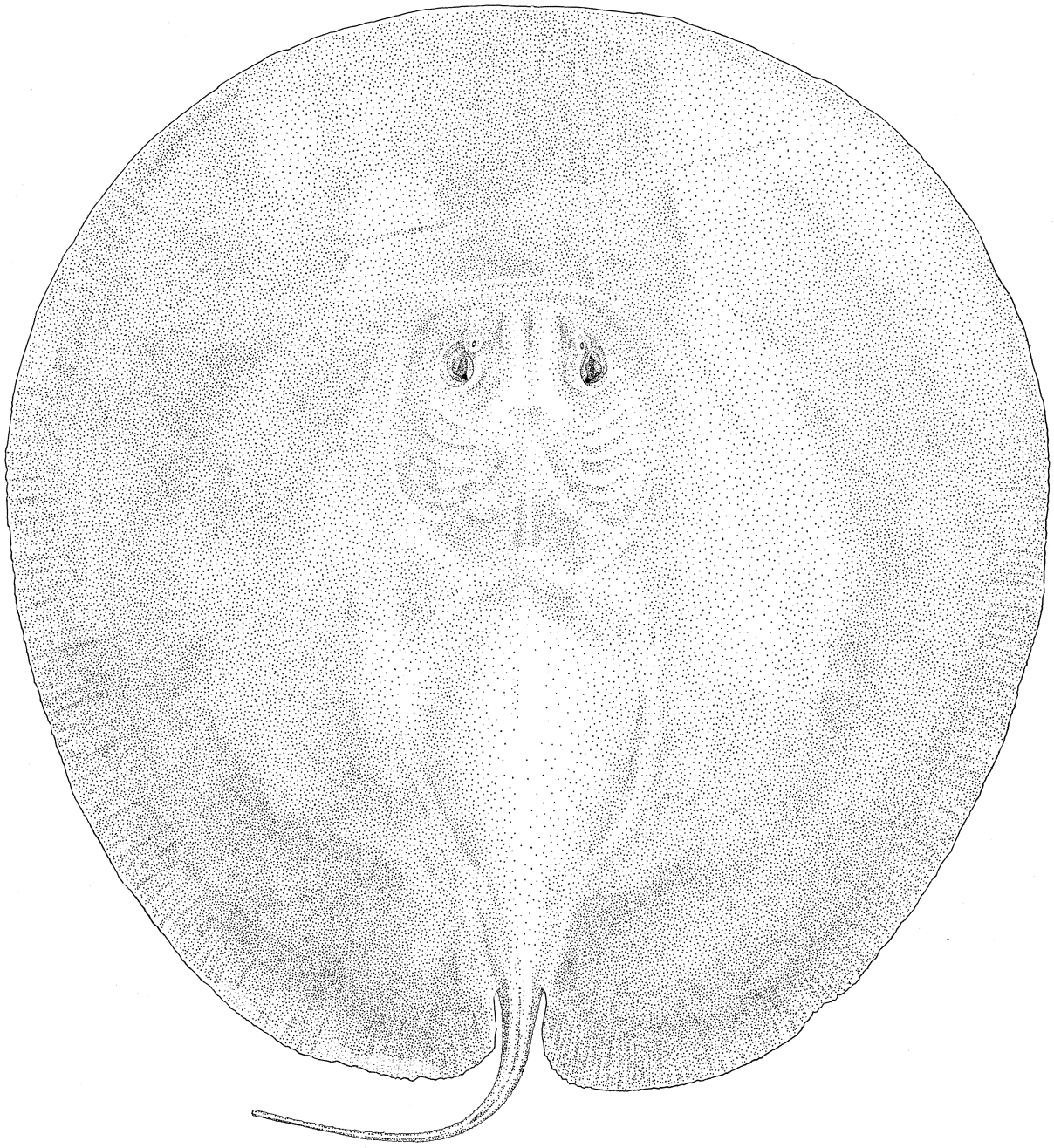

FIGURE 3. Illustration of paratype of *Heliotrygon gomesi*, n. sp., in dorsal view (based on AMNH 104988; see Figure 2).

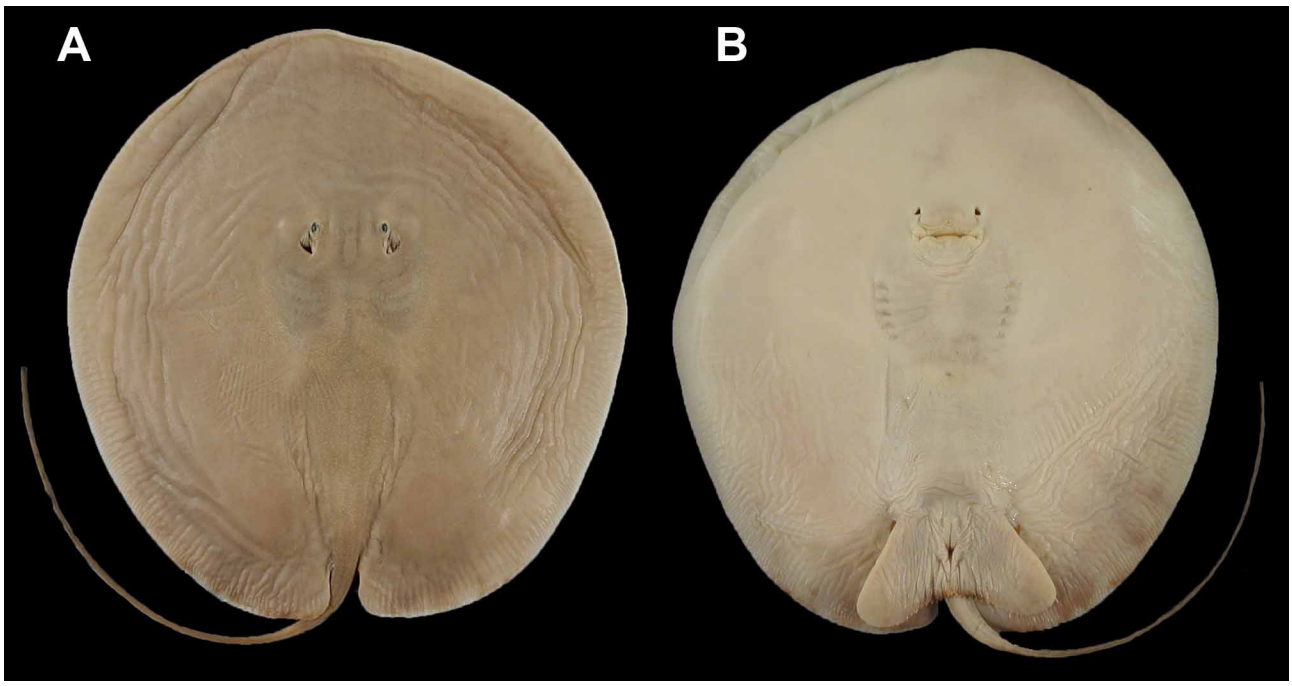

FIGURE 4. Paratype of *Heliotrygon gomesi*, n. sp., in dorsal (A) and ventral (B) views (ANSP 178017, preadult female, Rio Nanay, Rio Amazonas basin, 4.5 km west of Iquitos, Peru; 425 mm TL, 230 mm DL, and 224 mm DW).

TABLE 2. Meristc data for specimens of *Heliotrygon gomesi*, n. sp. A: MZUSP 104988 (holotype), adult female. B: MZUSP 108203 (paratype), juvenile female. C: CU 78485, preadult female. D: CU 78486, preadult female. E: AMNH 58402, preadult male.

CHARACTER	A	B	C	D	E	Range	Mode
precaudal vertebrae	30	31	31	31	30	30–31	31
caudal vertebrae	68	57	69	72	69	57–72	69
total vertebrae	98	88	100	103	99	88–103	-
diplospondylous vertebrae	68	57	65	68	64	57–68	68
upper tooth rows (radiograph)	27	-	23	25	22	22–27	-
lower tooth rows (radiograph)	32	-	24	24	23	23–32	24
upper tooth rows (specimen)	29	17	-	21	25	17–29	-
lower tooth rows (specimen)	27	18	-	21	23	18–27	-
propterygial radials	48	45	50	50	45	45–50	50
mesopterygial radials	24	23	23	25	25	23–25	23
metapterygial radials	38	35	37	39	39	35–39	39
total pectoral radials	110	103	110	114	109	103–114	110
pelvic radials	24	19	26	25	21	19–26	-

Pelvic fins completely concealed in dorsal view. Pelvic fins relatively short anteroposteriorly, much wider than long, and with undulating posterior margins. Pelvic fins broadest at more or less their midlength, with broadly oval apices. Tail very slender at base, its width more or less one-half of interorbital distance (tail width varying from 3.9 to 7.8% DW, x = 5.4% DW; holotype tail width 4.5% DW). Tail tapering to an elongated whip, usually greater than disc length but frequently broken, even in juveniles. Adults with much shorter tail, usually extending posteriorly a distance similar to width of pelvics. Tail with very slender, ridge-like lateral tail folds originating at base of tail and extending to more or less level of caudal sting; dorsal tail fold lacking but ventral tail fold present, ridge-like, originating posterior to level of caudal sting (more concealed in juveniles) and extending caudally a short distance.

Ventral tail-fold anteriorly wider, extending posteriorly as a very shallow ridge. Caudal sting very reduced, smaller or more or less equal to spiracle length. Caudal sting single in specimens, without sharp, lateral, posteriorly oriented serrations; serrations extremely reduced (observable with magnification) and blunt. Caudal sting very slender, usually less than 1 mm in width, and positioned just posteriorly to posterior margin of disc.

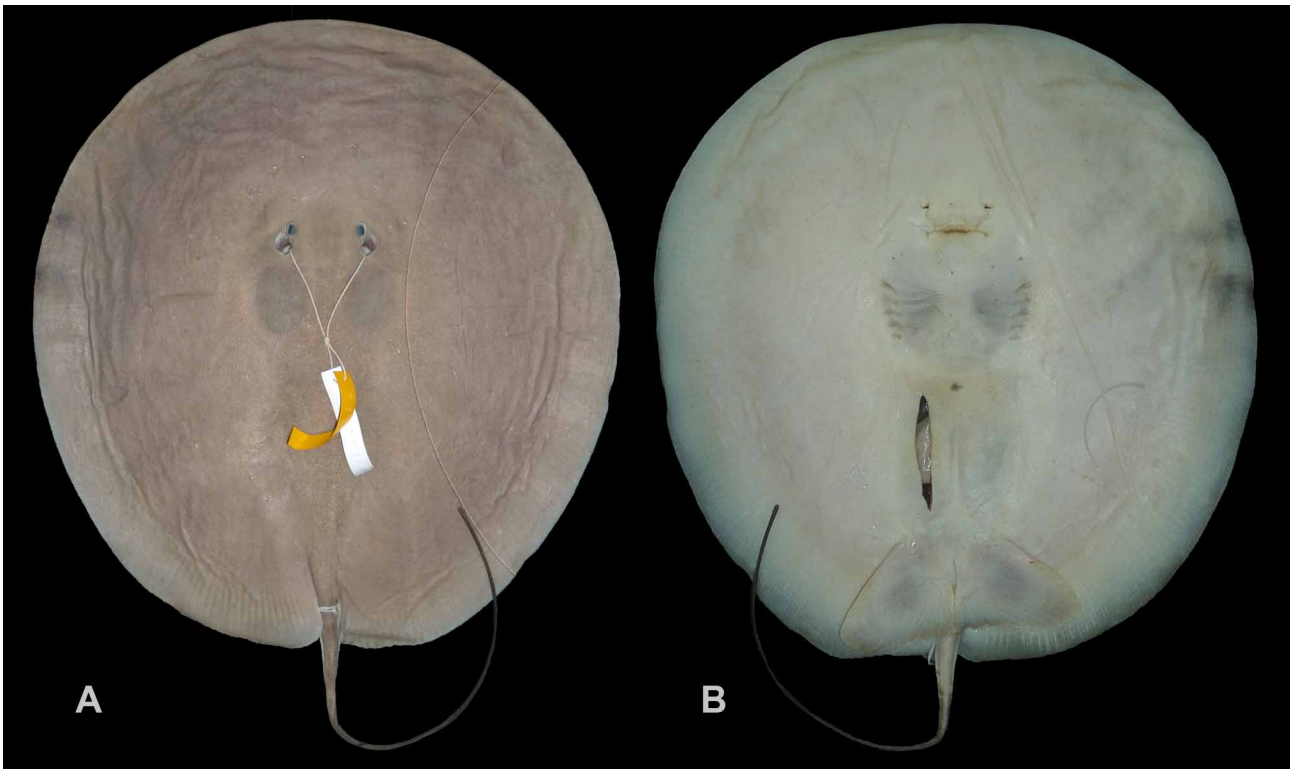

FIGURE 5. Paratype of *Heliotrygon gomesi*, n. sp., in dorsal (A) and ventral (B) views (MZUSP 108203, juvenile female, Rio Nanay, Rio Amazonas basin, Iquitos, Peru; 494 mm TL, 290 mm DL, and 269 mm DW). Dissected ventrally for parasites and for DNA extraction.

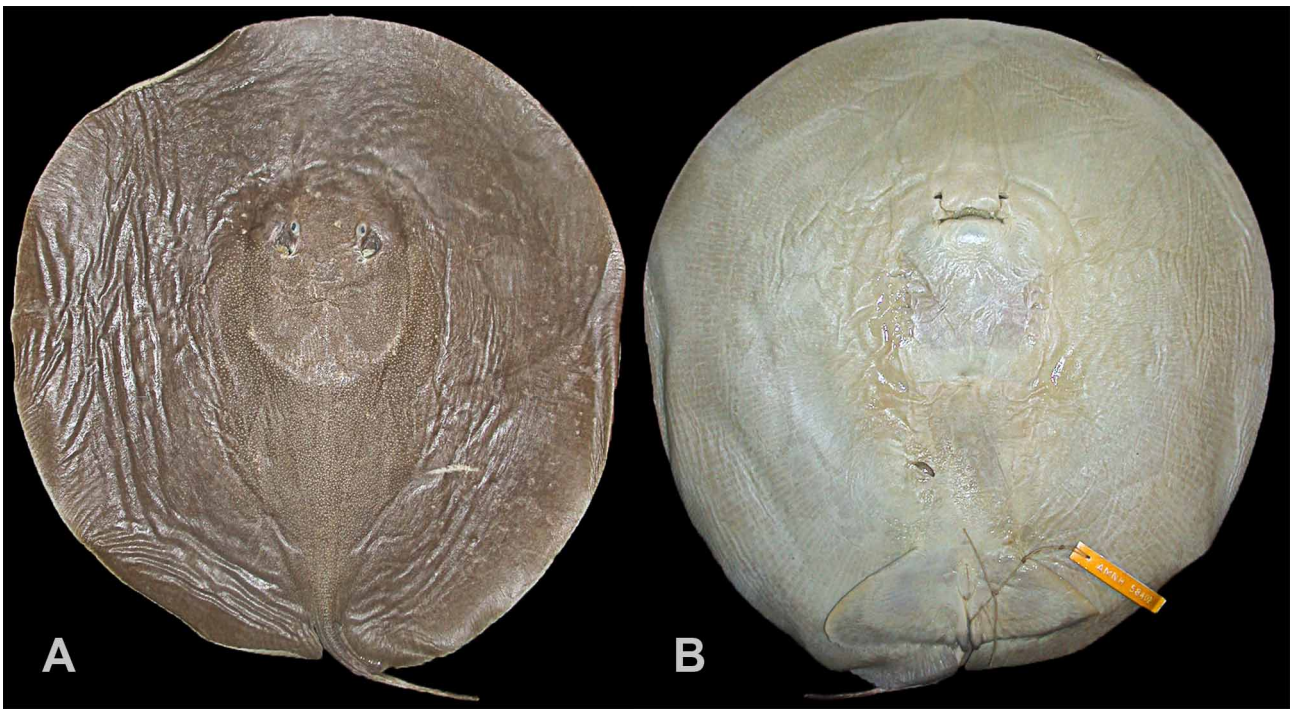

FIGURE 6. Specimen of *Heliotrygon gomesi*, n. sp., probably from Ecuador, in dorsal (A) and ventral (B) views (AMNH 58402, preadult male, 422 mm TL, 361 mm DL, and 345 mm DW).

FIGURE 7. Illustration of *Heliotrygon gomesi*, n. sp., in dorsal view (based on AMNH 58402; see Figure 6).

Coloration. Dorsal color varying from a uniform gray to light tan or brown background, generally without conspicuous spots, vermiculations, or other distinctive markings. Holotype with darker, irregularly shaped spots, smaller than eye diameter, over dorsal disc region; spots vary in size and distribution, but do not form conspicuous vermiculations, rosettes or other patterns; holotype dorsal coloration may be indicative of older, larger individuals. Ventral coloration uniform creamy white over most of ventral disc and pelvic fins. Some specimens with small, diffuse brownish or grayish patterns over posterior disc margins, base of tail region, and outer and posterior pelvic fins; other specimens without any markings on posterior disc and pelvic fins. Ventral surface of holotype with very slender part of posterior disc and pelvics with darker markings. Ventral tail coloration with brownish marks usually posterior to caudal sting; ventral tail region of holotype with a central whitish stripe. Distal tail region darker in comparison to base of tail.

Remarks. Identification to species level of larger specimens of *Heliotrygon* is easily accomplished by examining dorsal coloration. However, the proportional measurements in the diagnosis employed to separate *H. gomesi* from *H. rosai*, n. sp. (see also description below), are in need of further verification in additional material of both species. The length of the pelvic fin internal margin appears to be a slightly more consistent proportional character,

allowing for the separation of both species. The values provided above were extracted from all specimens and not only from the holotypes of both species, which are clearly distinct (2.1% DW in holotype of *H. gomesi*, and 4.6% DW in holotype of *H. rosai*). Taking all specimens into account, the differences in the mean concerning pelvic fin internal length is as great as the differences between the holotypes of both species (mean of 1.9% DW in *H. gomesi*, and 3.7% DW in *H. rosai*; Table 1).

The comparison of preorbital length proportions (and prenasal and preoral lengths) is slightly more difficult. The ranges of both species overlap for all specimens (32.6 to 35.7% DW in *H. gomesi*, and 31.0 to 34.2% DW in *H. rosai*), but directly comparing specimens of similar size, as with both holotypes (33.2% DW in holotype of *H. gomesi* and 31.0% DW in holotype of *H. rosai*), reveals slight distinctions. For example, preorbital snout length is relatively similar between MZUSP 108203 (*H. gomesi*) and MZUSP 108202 (*H. rosai*), even though the former is smaller in disc length (290 mm *vs*. 315 mm, respectively) and disc width (269 mm *vs*. 309 mm, respectively); preorbital snout length is 35.7% DW in MZUSP 108203 (*H. gomesi*) and 33.0% DW in MZUSP 108202 (*H. rosai*). Placing both individuals with their eyes aligned on same level, with ventral surfaces against each other, clearly shows that preorbital snout length is very similar even though the specimen of *H. rosai* is greater in disc length and width. In contrast, carrying out this exercise with a smaller specimen of *H. rosai* (MZUSP 108201) and the slightly larger MZUSP 108203 (*H. gomesi*) provided a different result, in which the preorbital snout length of the former was clearly smaller. Whether the snout length is truly diagnostic needs to be corroborated with the examination of more individuals from more localities. This is also true of tail width at base, which separates the holotypes quite easily, and certain specimens of similar proportions, but which proved more complex for all specimens examined.

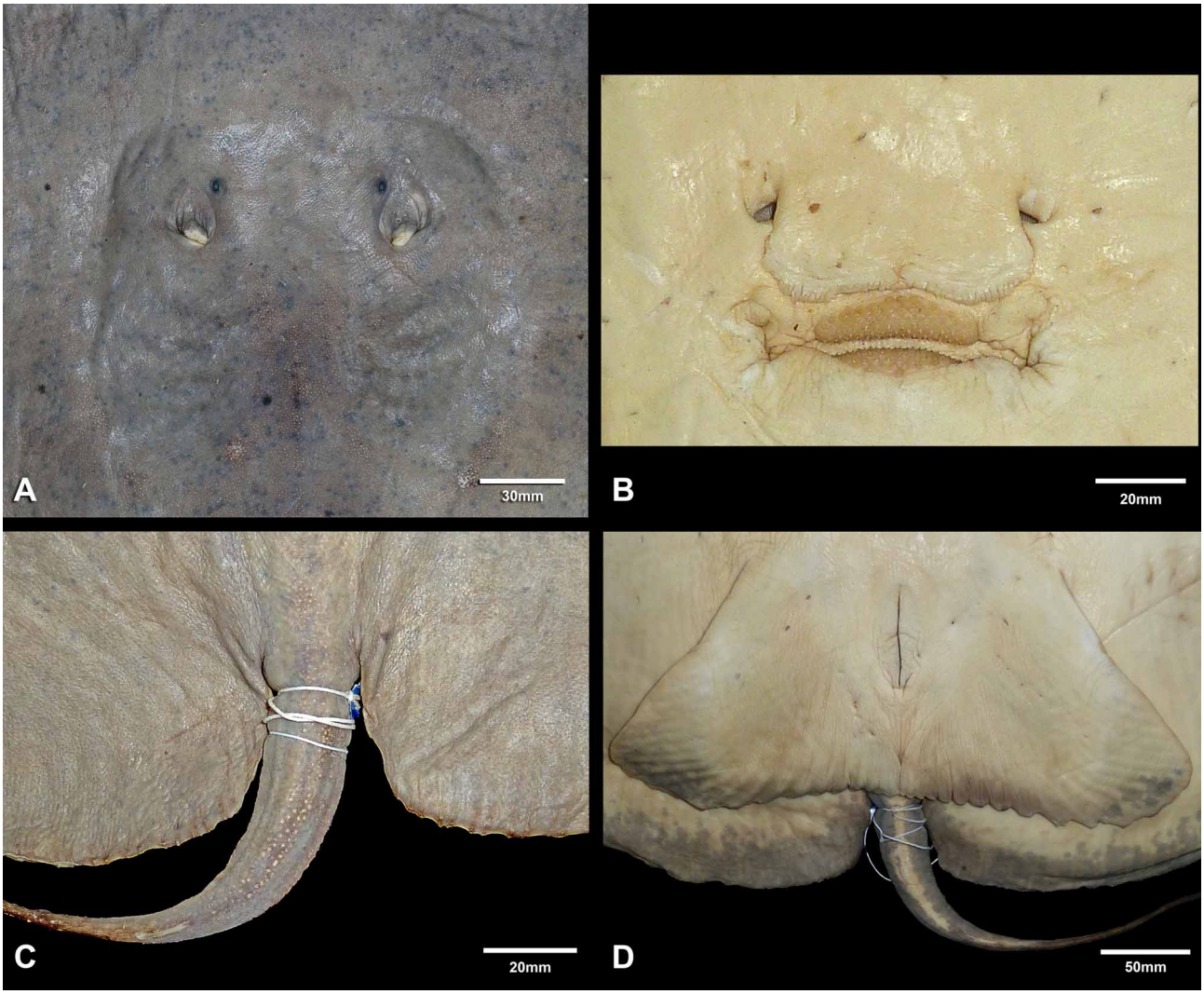

FIGURE 8. Morphological details of holotype of *Heliotrygon gomesi*, n. sp. A) Eyes and spiracles. B) Nasoral region. C) Dorsal tail region. D) Ventral view of pelvic fins and base of tail.

According to our material, male specimens of *H. gomesi* become sexually mature between 345 mm DW (AMNH 58402, 361 mm DL, a specimen with claspers protruding beyond posterior margin of pelvic fins, but claspers very slender and uncalcified), and 400 mm DW (ANSP 178014, 420 mm DL, a specimen with stout claspers that protrude well beyond posterior pelvic margin). Size of maturity for females, based on preserved material, is more difficult to discern. The holotype aborted a very late-term pup when captured, but sexual maturity must occur well before 624 mm in DW. In potamotrygonids, and elasmobranchs in general, females grow to proportionally much greater sizes than males (Araújo, 1998; Rosa et al., 2010), but sexual maturation in *H. gomesi* probably occurs for females at about 440 mm in DW.

FIGURE 9. Dorsal tail region depicting morphology of caudal sting of *Heliotrygon gomesi*, n. sp. A) AMNH 104988, paratype, adult female. B) MZUSP 104988, holotype, adult female. Notice faint, blunt serrations in (B). Anterior facing right. Scale = 5 mm.

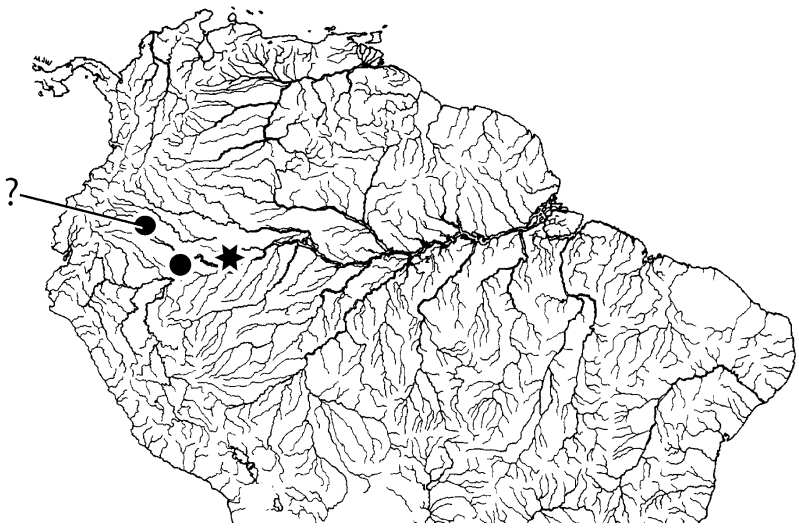

FIGURE 10. Geographic distribution of *Heliotrygon gomesi*, n. sp. Star depicts approximate locality of holotype. Question mark represents AMNH 58402 (Ecuador).

Geographic distribution. *Heliotrygon gomesi* is distributed in the upper Rio Amazonas basin according to our material (Figure 10), but enters, we suspect, the lower reaches of most major tributaries and the lower Rio Amazonas basin as well. Its distribution is very similar to that of *Plesiotrygon iwamae* (Rosa et al., 1987; Carvalho et al., 2003).

Etymology. This new species honors Ulisses L. Gomes, a pioneer in the study of elasmobranch morphology and systematics in Brazil, and an esteemed colleague and collaborator of the first author.

Proposed common name. Gomes's round ray (also referred to as "china" ray in the aquarium trade).

***Heliotrygon rosai*, n. sp.**
Figures 11–16; Tables 3–4

Holotype. MZUSP 104996, adult male, Baía de Marajó, 0°55'34''S, 48°17'25''W, Colares, Pará, Brazil, coll. P. C.-Almeida. (Figures 11, 16).

Paratypes. (4 specimens). AMNH 251885, preadult male, Rio Nanay, Rio Amazonas basin, Iquitos, Loreto, Peru (aquarium trade specimen) (Figures 12, 13); MZUSP 108200, juvenile female, Rio Nanay, Rio Amazonas basin, Iquitos, Loreto, Peru, coll. F. Marques (PU 09-06), 17.x.2009 (Figure 14); MZUSP 108201, juvenile female, same locality and collection date as MZUSP 108200, coll. F. Marques (PU 09-05) (Figure 14); MZUSP 108202, juvenile male, same locality as MZUSP 108200, coll. F. Marques (PU 09-19), 18.x.2009 (Figure 14).

Other material. (2 specimens). MZUSP 63604, juvenile male, Rio Purus, 1.1 km downriver from São Tomé, 03°48'10"S, 061°25'17"W, Amazonas state, Brazil, coll. S. Jewett & collaborators (ACFSLJ 93010), 25.x.1993 (Figure 15); MZUSP 108295, adult male, Baía de Marajó, Colares, Pará, Brazil, 4.xi.2003, coll. F. Marques & P. C.-Almeida (PA03-49) (very large specimen, between 700 and 800 mm DW, heavily dissected, missing lateral disc, snout and tail regions).

Diagnosis. A species of *Heliotrygon* diagnosed by its unique dorsal color pattern, composed of numerous white to creamy-white vermiculate markings over a light brown, tan or gray background color. *Heliotrygon rosai* is tentatively further separated from *H. gomesi* by presenting a slightly more slender tail width at base (5.5% DW in holotype of *H. rosai* vs. 4.5% DW in holotype of *H. gomesi*), slightly greater preorbital snout length (31% DW in holotype of *H. rosai vs*. 33.2% DW in holotype of *H. gomesi*), and smaller pectoral axil to pelvic inner length (4.6% DW in holotype of *H. rosai*, ranging from 1.3 to 4.9% DW in all specimens, with a mean of 3.7% DW *vs*. 2.1% DW in holotype of *H. gomesi*, and ranging from 1.0 to 3.3% DW in all specimens, with a mean of 1.9% DW).

Description. Measurements are presented as raw data in mm and percentages of DW (Table 3); meristic characters are provided in Table 4. As with *H. gomesi*, the description is based on all specimens, with significant features of the holotype separately mentioned. For the description below, refer to Figures 11–16.

External morphology. Disc flat, its greatest height more or less equal to interorbital space (less than one-tenth of disc width). Disc extremely circular, widest at midlength near, or just anterior to, scapulocoracoid. Disc length varying from 101.9% to 108% DW (x = 104.9% DW; in holotype disc length 104.7% DW). Snout broadly rounded, elongated, and convex. Snout length about four times interorbital distance. Preorbital snout length ranging from 31 to 34.2 % DW (x = 33.1% DW; in holotype, preorbital snout length 31% DW). Prenasal snout length ranging between 26.5 and 29.4% DW (x = 28.3% DW; in holotype, prenasal snout length 26.5% DW). Preoral snout varying from 29.6% to 34.2% DW (x =32.3% DW; in holotype, preoral snout length 29.6% DW). Snout with strongly circular anterior margin, and with minute rostral knob protruding from anterior disc (more evident in juveniles). Posterior disc region slightly more oval than anterior disc region.

Eyes very small, smaller than spiracles, and not protruding significantly above disc. Spiracles closely adjacent to eyes, rhomboidal. Spiracles about as wide as long, without elevated spiracular rims or central knob posteriorly. Mouth opening relatively straight across, its width close to one-half distance between first gill slits, and about equal to internarial distance. Posterior profile of lower jaw presenting rugose grooves; labial folds absent. Outer corners of mouth also with marked grooves. Nostrils about equal or slightly smaller than eye-diameter; nostrils circular. Nasal curtain medially notched posteriorly, with posterior margin greatly fringed. Lateral margins of nasal curtain reaching to nostril midlength. Teeth externally visible with mouth closed; tooth row counts 28/28 in holotype. Adult males with sharp, pointed cusps; cusps in adult females smaller, less pointed and more evenly triangular. Shallow integumental rugae present ventrally posterior to mouth and anterior to branchial basket region. Branchial basket relatively short anteroposteriorly, much shorter than wide (branchial basket length ranges from 8.2 to 11.5%

DW, whereas distance between first gill openings varies between 17.3 to 20.9% DW). Distance between first gill slits slightly greater than distance between fifth gill slits. Gill openings with slightly curved gill flap; fifth gill slit smallest, slightly more obliquely positioned compared to first gill slit.

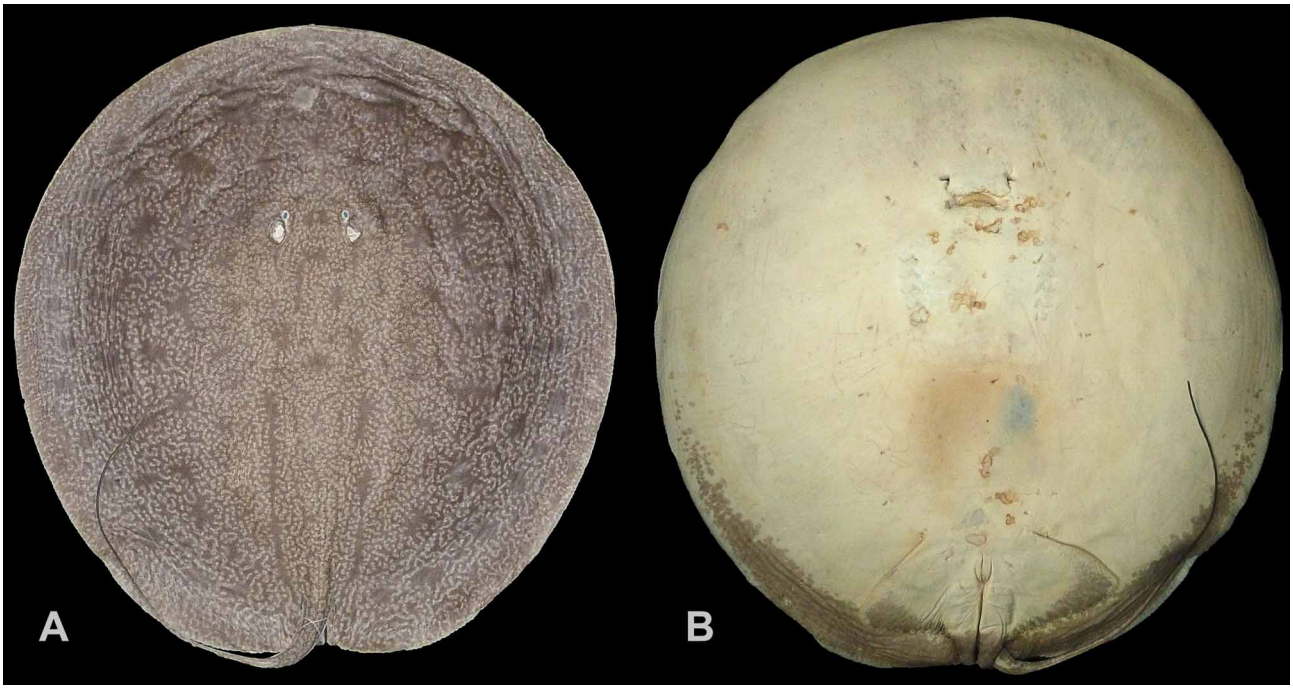

FIGURE 11. Holotype of *Heliotrygon rosai*, n. sp., in dorsal (A) and ventral (B) views (MZUSP 104996, adult male, Baía de Marajó, Pará state, Brazil; 984 mm TL, 604 mm DL, 577 mm DW).

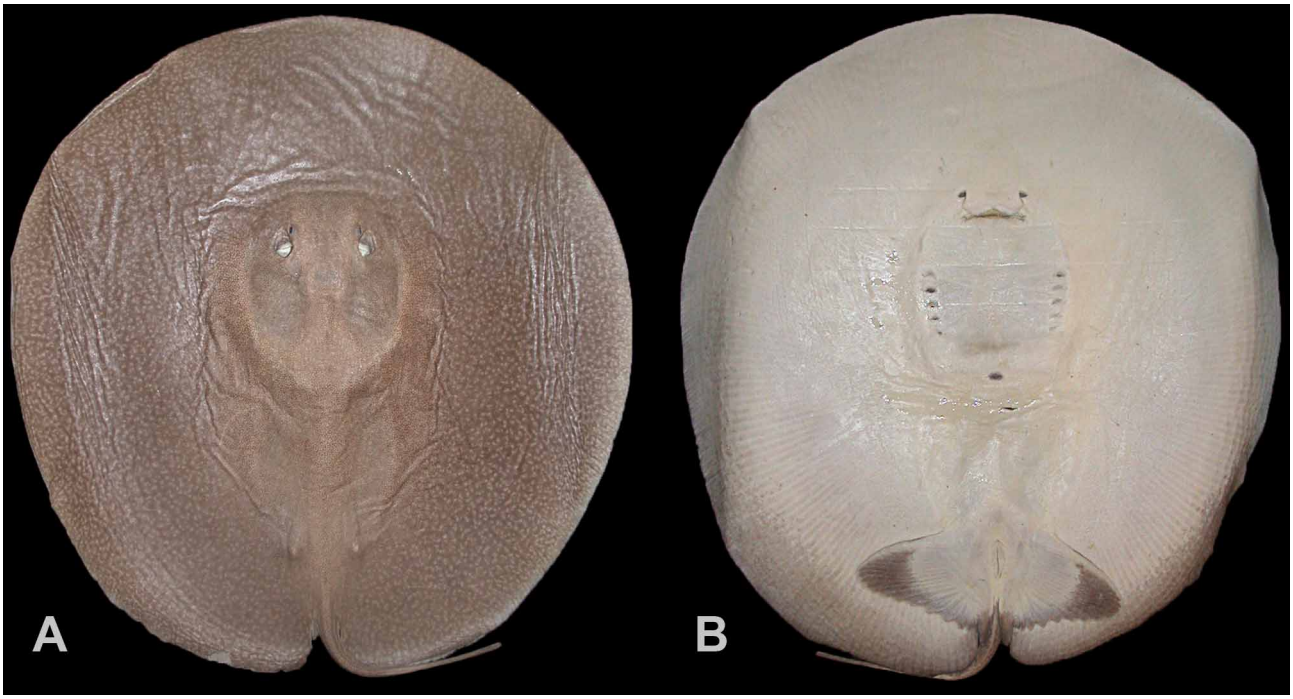

FIGURE 12. Paratype of *Heliotrygon rosai*, n. sp., in dorsal (A) and ventral (B) views (AMNH 251885, preadult male, Rio Nanay, Rio Amazonas basin, Iquitos, Peru; 599 mm TL, 500 mm DL, 483 mm DW).

Pelvic fins completely hidden in dorsal view, relatively short anteroposteriorly (much wider than long), and with undulating posterior margins. Pelvic fins broadest at more or less their midlength, with broadly oval apices. Tail very slender at base, its width more or less one-half of interorbital distance (tail width ranging between 4.9% and 5.8% DW, x = 5.3%; in holotype, tail width 5.6% DW). Tail tapering to an elongated whip, usually greater than

disc length but frequently broken, even in juveniles. Adults with much shorter tail, usually extending posteriorly a distance similar to width of pelvics. Tail with very slender, ridge-like lateral tail folds originating at base of tail and extending to more or less level of caudal sting; dorsal tail fold lacking in most specimens but present in holotype; ventral tail fold present in holotype as low ridge, originating posterior to level of caudal sting and extending caudally as a very low keel; ventral keel absent in some other specimens. Caudal sting significantly reduced, smaller or more or less equal to spiracle length. Caudal sting single in specimens in which they were not lost, without sharp, lateral, posteriorly oriented serrations; serrations extremely reduced in size and blunt. Caudal sting very slender, usually less than 1 mm in width, and positioned just posteriorly to posterior margin of disc.

FIGURE 13. Illustration of paratype of *Heliotrygon rosai*, n. sp., in dorsal view (based on AMNH 251885; see Figure 12).

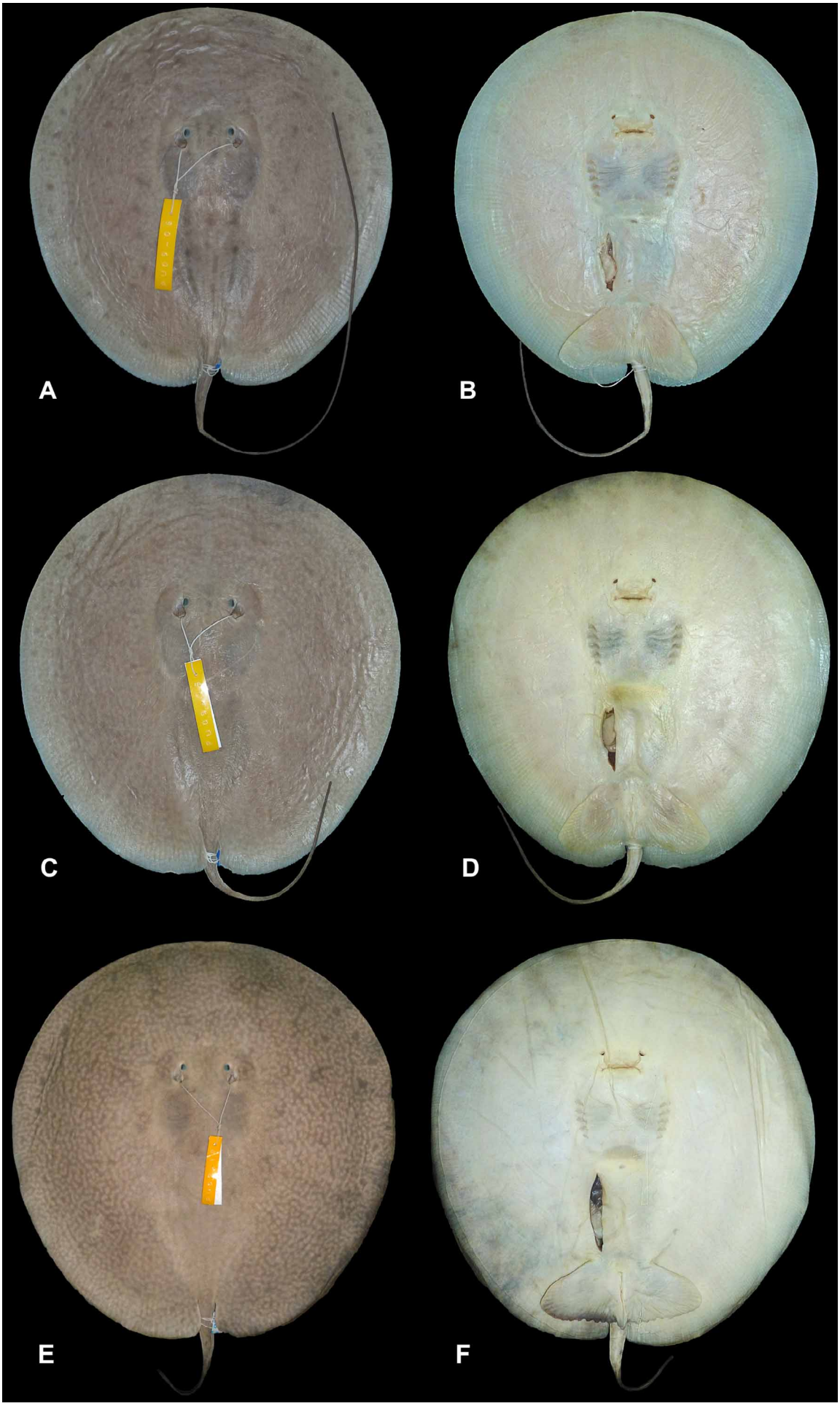
A
B
C
D
E
F

FIGURE 14. Paratypes of *Heliotrygon rosai*, n. sp., showing minor dorsal color variation, in dorsal (A, C, E) and ventral (B, D, F) views. A, B) MZUSP 108200, juvenile female, Rio Nanay, Rio Amazonas basin, Iquitos, Peru (500 mm TL, 215 mm DL, 206 mm DW). C, D) MZUSP 108201, juvenile female, same locality (362 mm TL, 244 mm DL, 226 mm DW). E, F) MZUSP 108202, juvenile male (404 mm TL, 315 mm DL, 309 mm DW).

Clasper dorsoventrally depressed (Figure 24), relatively short (length 12.1% DW) and stout, wide at base and narrowing only slightly distally, with rounded to more or less straight extremity. Clasper groove beginning proximally, well before level of posterior margin of pelvics. Anterior half of clasper groove running obliquely from inner margin to outer margin of clasper. Posterior half of clasper groove curving inward at level of dorsal pseudosiphon, reaching midline caudal to posterior border of dorsal pseudosiphon, and extending to clasper tip. Dorsal pseudosiphon small in relation to clasper length, near inner clasper edge. Dorsal pseudosiphon elliptical, and obliquely oriented in relation to midline. Ventral pseudosiphon well developed, located at lateral distal edge of clasper.

Coloration. Dorsal coloration somewhat variable among specimens, more so than in *H. gomesi*. Dorsal coloration composed of numerous beige to whitish vermicular markings forming complex, reticular patterns over a brown, tan or gray background color. Vermiculations may delimit circular areas of only background color, usually smaller than interorbital distance, on dorsal disc region (as in holotype; Figure 11). These brownish blotches distributed in a regular fashion over disc, more or less evenly spaced apart, and diminishing in size near outer disc margins. Specimen AMNH 104996 (preadult male paratype) lacks brownish blotches on dorsal disc, with dorsal color composed solely of more regularly distributed vermiculate markings (Figure 12). Variation in dorsal color pattern not a function of gender (Figure 14). Conspicuous dorsal coloration pattern also over pelvic fins and base of tail region. Ventral coloration mostly a uniform, creamy-white, but with darker blotches on posterior disc margins, ventral tail region and pelvic fins (both posteriorly and laterally) in larger specimens. Darker posterior disc margins reach anteriorly to posterior third of disc length in holotype. Pelvic fin ventral color varied among specimens as some present faint markings whereas others present stronger patterns. Ventral tail coloration darker posteriorly.

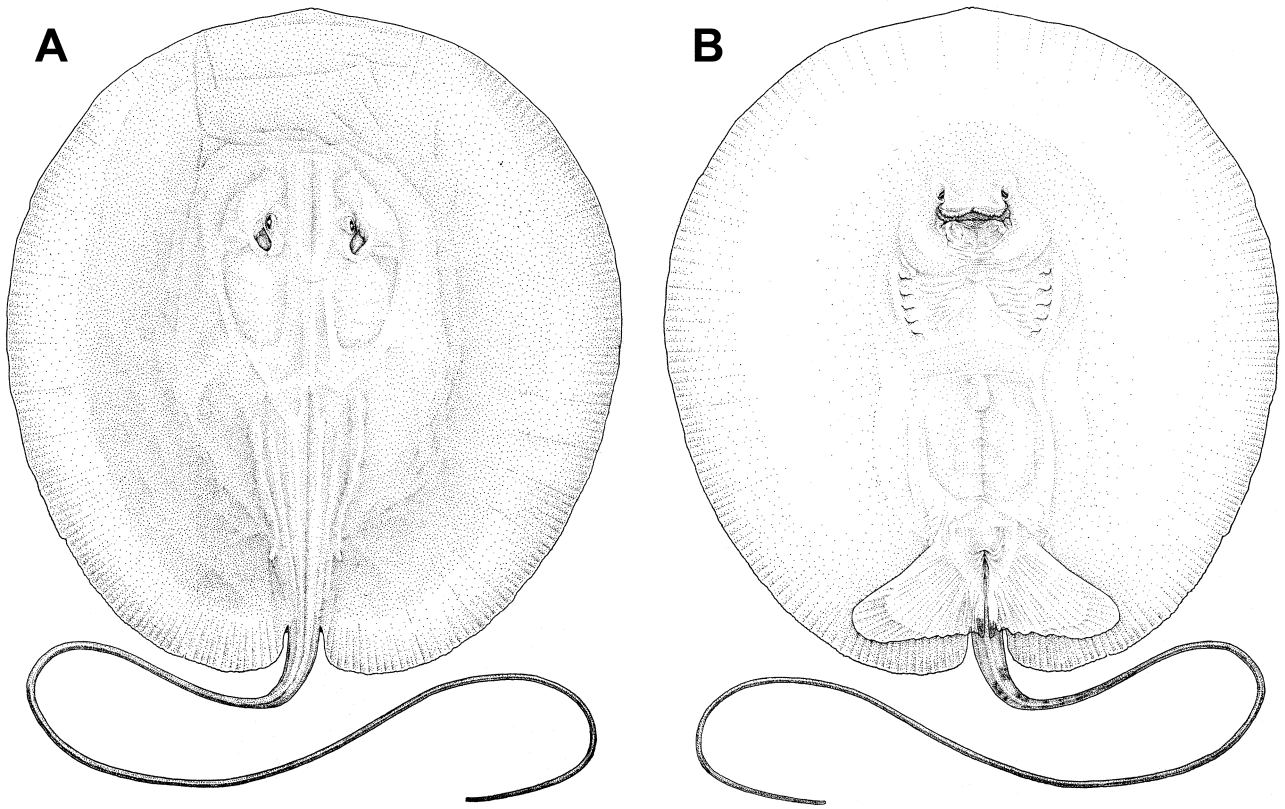

FIGURE 15. Illustration of *Heliotrygon rosai*, n. sp., in dorsal (A) and ventral (B) views (MZUSP 63604, juvenile male, Rio Purus, Amazonas state, Brazil, 680 mm TL, 247 mm DL, 231 mm DW). Note that dorsal color pattern has faded significantly in this specimen.

TABLE 3. Measurements of specimens of *Heliotrygon rosai*, n. sp. A: MZUSP 104996 (holotype), adult male. B: AMNH 251885 (paratype), preadult male. C: MZUSP 108200 (paratype), juvenile female. D: MZUSP 108201 (paratype), juvenile female. E: MZUSP 108202 (paratype), juvenile male. F: MZUSP 63604, juvenile male. *x*: mean. SD: standard deviation.

PARAMETER	A		B		C		D		E		F		RANGE	*x*		SD	
	mm	% DW	mm	% DW	mm	% DW	mm	% DW	mm	% DW	mm	% DW	% DW	mm	% DW	mm	% DW
total length (TL)	984.0	-	599.0	-	500.0	-	362.0	-	404.0	-	680.0	-	-	588.2	-	227.2	-
disc length (DL)	604.0	104.7	500.0	103.5	215.0	104.4	244.0	108.0	315.0	101.9	247.0	106.9	101.9–108.0	354.2	104.9	160.1	2.2
disc width (DW)	577.0	100.0	483.0	100.0	206.0	100.0	226.0	100.0	309.0	100.0	231.0	100.0	-	338.7	-	155.2	-
interorbital distance	48.0	8.3	51.0	10.6	22.0	10.7	23.0	10.2	30.0	9.7	24.0	10.4	8.3–10.7	33.0	10.0	13.1	0.9
interspiracular distance	56.0	9.7	55.0	11.4	32.0	15.5	32.0	14.2	34.0	11.0	33.0	14.3	9.7–15.5	40.3	12.7	11.8	2.3
eye length	6.0	1.0	6.0	1.2	3.0	1.5	2.0	0.9	5.0	1.6	4.0	1.7	0.9–1.7	4.3	1.3	1.6	0.3
spiracle length	27.0	4.7	29.0	6.0	7.0	3.4	9.0	4.0	12.0	3.9	7.0	3.0	3.0–6.0	15.2	4.2	10.1	1.1
preorbital length	179.0	31.0	165.0	34.2	70.0	34.0	76.0	33.6	102.0	33.0	76.0	32.9	31.0–34.2	111.3	33.1	48.5	1.1
prenasal length	153.0	26.5	142.0	29.4	60.0	29.1	63.0	27.9	84.0	27.2	68.0	29.4	26.5–29.4	95.0	28.3	41.6	1.2
preoral length	171.0	29.6	160.0	33.1	70.0	34.0	76.0	33.6	96.0	31.1	79.0	34.2	29.6–34.2	108.7	32.6	45.0	1.8
internarial distance	49.0	8.5	48.0	9.9	21.0	10.2	21.0	9.3	26.0	8.4	20.0	8.7	8.4–10.2	30.8	9.2	13.8	0.8
mouth width	56.0	9.7	51.0	10.6	22.0	10.7	23.0	10.2	28.0	9.1	22.0	9.5	9.1–10.7	33.7	9.9	15.6	0.6
distance between 1st gill slits	100.0	17.3	89.0	18.4	43.0	20.9	46.0	20.4	58.0	18.8	45.0	19.5	17.3–20.9	63.5	19.2	24.8	1.3
distance between 5th gill slits	92.0	15.9	84.0	17.4	38.0	18.4	42.0	18.6	53.0	17.2	38.0	16.5	15.9–18.6	57.8	17.3	24.1	1.0
branchial basket length	58.0	10.1	46.0	9.5	23.0	11.2	26.0	11.5	30.0	9.7	19.0	8.2	8.2–11.5	33.7	10.0	15.1	1.2
pelvic fin anterior margin length	96.0	16.6	87.0	18.0	40.0	19.4	39.0	17.3	50.0	16.2	37.0	16.0	16.0–19.4	58.2	17.3	26.4	1.3
pelvic fin width	231.0	40.0	203.0	42.0	85.0	41.3	95.0	42.0	125.0	40.5	91.0	39.4	39.4–42.0	138.3	40.9	63.1	1.1
clasper external length	36.0	6.2	27.0	5.6	-	-	-	-	12.0	3.9	7.0	3.0	3.0–6.2	20.5	4.7	13.4	1.5
clasper internal length	87.0	15.1	60.0	12.4	-	-	-	-	27.0	8.7	20.0	8.7	8.7–15.1	48.5	11.2	31.0	3.1
distance between cloaca and tail tip	480.0	83.2	204.0	42.2	312.0	151.5	151.0	66.8	139.0	45.0	468.0	202.6	42.2–202.6	292.3	98.5	153.5	64.7
tail width	32.0	5.5	28.0	5.8	10.0	4.9	11.0	4.9	17.0	5.5	12.0	5.2	4.8–5.8	18.3	5.3	9.4	0.4
snout to cloaca distance	476.0	82.5	384.0	79.5	179.0	86.9	193.0	85.4	256.0	82.8	199.0	86.1	79.6–86.9	281.2	83.9	121.8	2.8
pectoral to posterior pelvic length	28.0	4.9	-	-	7.0	3.4	10.0	4.4	14.0	4.5	3.0	1.3	1.3–4.9	12.4	3.7	9.6	1.4
distance from cloaca to sting origin	-	-	-	-	-	-	-	-	-	-	-	-	-	-	-	-	-
sting length	-	-	-	-	-	-	-	-	-	-	-	-	-	-	-	-	-
sting width	-	-	-	-	-	-	-	-	-	-	-	-	-	-	-	-	-

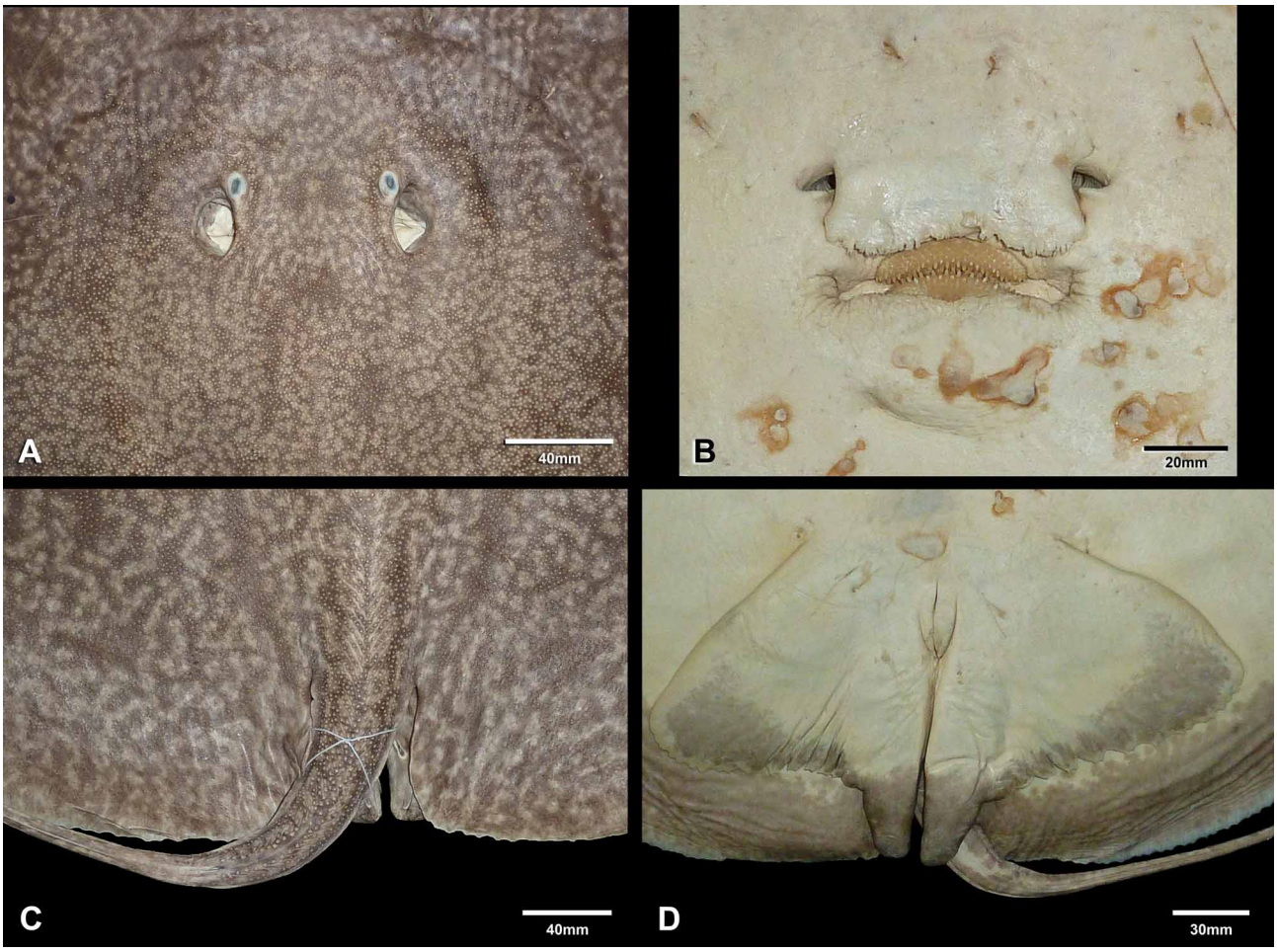

FIGURE 16. Morphological details of holotype of *Heliotrygon rosai*, n. sp. A) Eyes and spiracles. B) Nasoral region. C) Dorsal tail region (claspers barely noticeable; specimen is an adult). D) Ventral view of pelvic fins and base of tail.

TABLE 4. Meristc data for specimens of *Heliotrygon rosai*, n. sp. A: MZUSP 104996 (holotype), adult male. B: AMNH 251885 (paratype), preadult male. C: MZUSP 108200 (paratype), juvenile female. D: MZUSP 108201 (paratype), juvenile female. E: MZUSP 108202 (paratype), juvenile male. F: MZUSP 63064, juvenile male.

CHARACTER	A	B	C	D	E	F	Range	Mode
precaudal vertebrae	32	29	31	32	28	31	28–32	32
caudal vertebrae	71	71	50	56	65	64	50–71	71
total vertebrae	103	100	81	88	93	95	81–103	-
diplospondylous vertebrae	70	66	-	51	62	60	51–70	-
upper tooth rows (radiograph)	26	-	-	-	-	21	21–26	-
lower tooth rows (radiograph)	28	-	-	-	-	21	21–28	-
upper tooth rows (specimen)	28	19	11	18	18	20	11–28	18
lower tooth rows (specimen)	28	19	10	18	18	21	10–28	18
propterygial radials	50	47	46	42	46	49	42–50	46
mesopterygial radials	26	25	26	25	26	23	25–26	26
metapterygial radials	37	37	36	36	33	38	33–38	37
total pectoral radials	113	-	108	103	105	111	103–113	-
pelvic radials	21	21	18	18	17	22	17–22	21

Remarks. For comments on identifying both *H. rosai* and *H. gomesi* based on proportional measurements, see Remarks for the latter species, above. Information on sexual maturity for *H. rosai* females, based on preserved material is not as clear as in *H. gomesi*, as the larger specimens are male. The holotype is clearly sexually mature, but the large paratype (AMNH 281885) has claspers that are still flexible, easily bent dorsally, not as stout and firm as in the holotype. Sexual maturity for males therefore occurs between 483 and 577 mm DW (and 500 and 604 mm DL).

In terms of the size that these stingrays may reach, we examined and dissected a specimen (MZUSP 108295) that had both sides of the disc removed, along with the tail and snout region. This specimen is clearly much larger than the adult male holotype and also much thicker at the scapulocoracoid region. The measurements obtained from this specimen are as follows: interorbital width: 59 mm; interspiracular width: 67 mm; eye length: 9 mm; spiracle length: 27 mm; mouth width: 65 mm; distance between first gill slits: 121 mm; distance between fifth gill slits: 110 mm; branchial basket length: 61 mm; pelvic fin anterior width: 92 mm; and tail width at base: 28 mm. From the relative proportions deduced from some of these measurements, in particular interspiracular and interorbital distances and mouth width (which is not easily distorted even in a mutilated specimen), and compared to other specimens in hand, we may infer that this specimen may have been around 700 to 750 mm in DW, and slightly greater in DL. This is no surprise if we examine the very large sizes reached in the closely related *Paratrygon aiereba* (specimens greater than 100 cm in DW have been reported).

The holotype of *H. rosai* had ingested a catfish (Siluriformes, possibly a doradid) about the size of the metapterygium (visible in radiographs). The catfish was ingested whole, head first, and is relatively intact in the abdominal cavity.

Geographic distribution. *Heliotrygon rosai* is known from the upper, mid and lower Rio Amazonas basin, and probably also enters, we believe, the lower reaches of its major tributaries (Figure 17). As with *H. gomesi*, its distribution is similar to that of *Plesiotrygon iwamae* (Rosa et al., 1987; Carvalho et al., 2003).

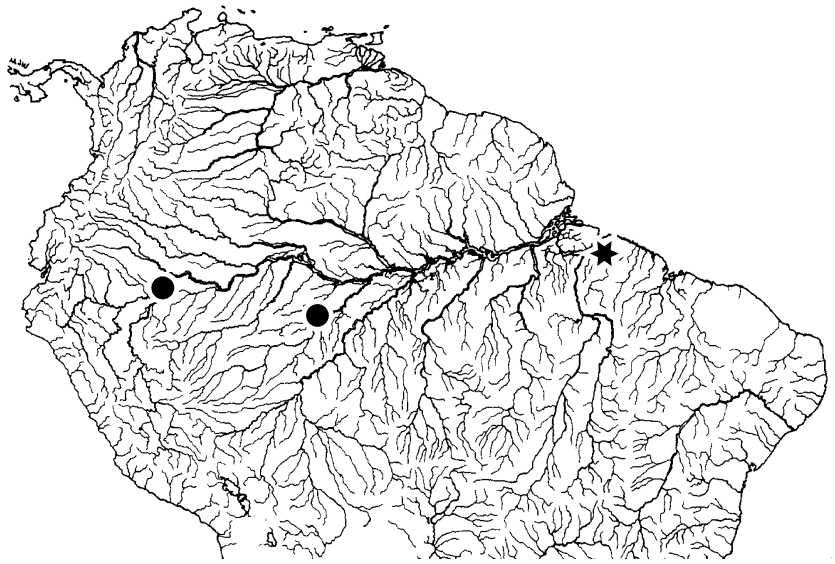

FIGURE 17. Geographic distribution of *Heliotrygon rosai*, n. sp. Star depicts approximate locality of holotype.

Etymology. This new species is named after Ricardo S. Rosa, whose excellent revision of potamotrygonids (Rosa, 1985a) represents a landmark in our understanding of the taxonomy and diversity of this family.

Proposed common name. Rosa's round ray (also referred to as "coly" ray in the aquarium trade).

Morphology of *Heliotrygon*

The description of dermal denticles that follows is based on *H. rosai* (MZUSP 108295), but the ventral lateral-line canals are based on *H. gomesi* (MZUSP 108203). Clasper skeleton is described based on adult claspers of *H. rosai* (MZUSP 108295), as adult claspers of *H. gomesi* were not available for dissection, but clasper external morphol-

ogy (included above in the account on external morphology of *H. rosai*) was based on the holotype (MZUSP 104996). Description of cranial muscles is also based on *H. rosai* (MZUSP 108295).

Dermal denticles. (Figures 9A, 18, 23A, 23C). Denticles small (much smaller than eye-diameter), evenly distributed, and present on dorsal disc region mostly over mid- and posterior disc and base of tail. Denticles very minute and low. Larger spines and thorns entirely absent. On tail region, denticles more intensely grouped together at tail base, with scattered denticles occurring on lateral tail aspects, and sporadically far distally on tail. Microscopically, dermal denticles on dorsal disc region of a single morphotype, with an oval-shaped crown and averaging around 0.5 mm in length. Posteriorly on the crown, two parallel crown keels originate from a coronal dichotomy. The opposite side of the crown is round to oval. Denticle basal plate oval, interrupted in the coronal keel area. A small basal keel occurs in variable numbers, being sometimes absent. In lateral view, denticle base and basal keels visible. Denticles on dorsal and lateral tail regions with slightly different morphology from dorsal middisc (Figure 9A), star-shaped in dorsal view, and with radiating keels converging on denticle apex.

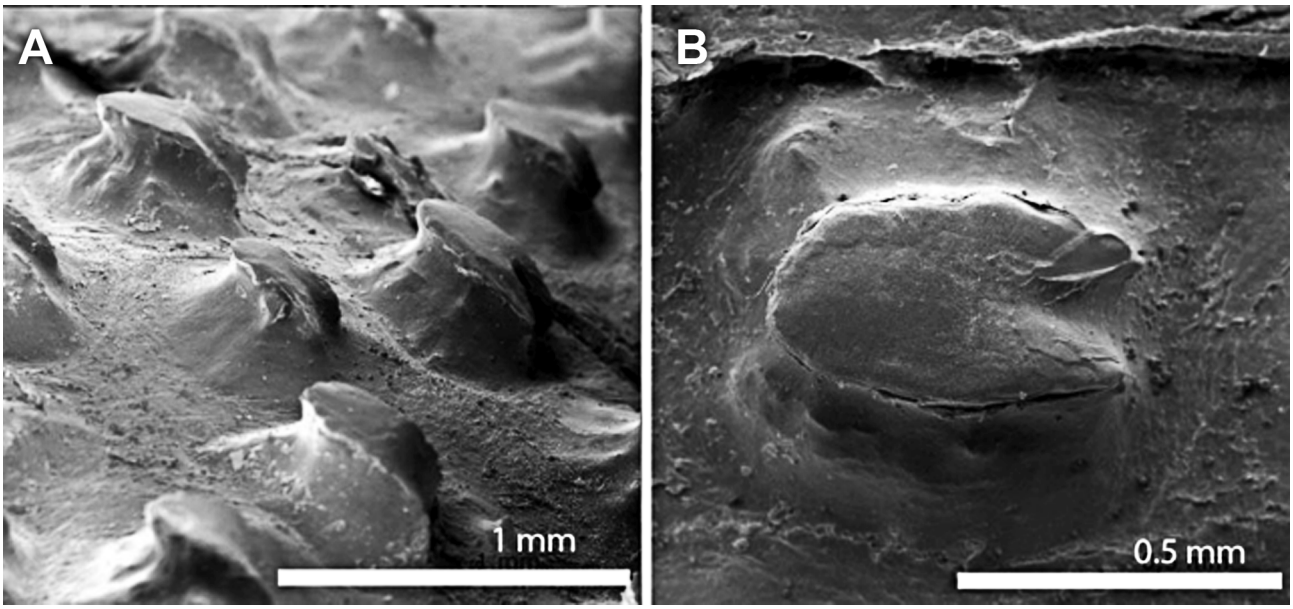

FIGURE 18. Dermal denticles of *Heliotrygon rosai*, n. sp. (from MZUSP 108295, adult male). A) Denticles from anterior, central disc region (anterior facing right). B) Single denticle in higher magnification (anterior facing left).

Ventral lateral-line canals. (Figure 19). Ventral lateral-line canals present a complex, honeycomb-like pattern on anterolateral disc region. Suborbital component of the infraorbital canal highly reticulated and web-like, delimiting a network of small loops of varying sizes. Suborbital component covering most of anterolateral disc region, from level of fourth gill opening to outer anterolateral disc margin. Loops of suborbital greater and more elongated posteriorly, reducing in size outwardly toward disc margins, becoming very small close to anterolateral disc margins near hyomandibular canal. Hyomandibular canal subdivided into jugular and subpleural components. Hyomandibular canal bordering anterolateral disc margins, running more or less parallel to disc margin. Subpleural component of the hyomandibular canal deflects inward toward disc center more or less at level of third gill opening, where it delimits irregular circular to oval loops. Subpleural extends posteriorly to posterior one-fourth of disc. Anterolaterally the hyomandibular canal gives off numerous small, perpendicular branches toward disc outer margin (the anterior subpleural tubules). Supraorbital canal extends from nasal curtain region posteriorly before deflecting to form slender, elongated anterior loop. Posteriorly, supraorbital canal reaches slightly caudal to level of mouth. Prenasal canal extends anteriorly in a more or less parallel fashion from nasal curtain to anterior disc. The jugular component of the hyomandibular canal reaches posteriorly, arching around branchial basket from junction with suborbital and supraorbital canal, to reach subpleural component at posterior three-fourths of disc.

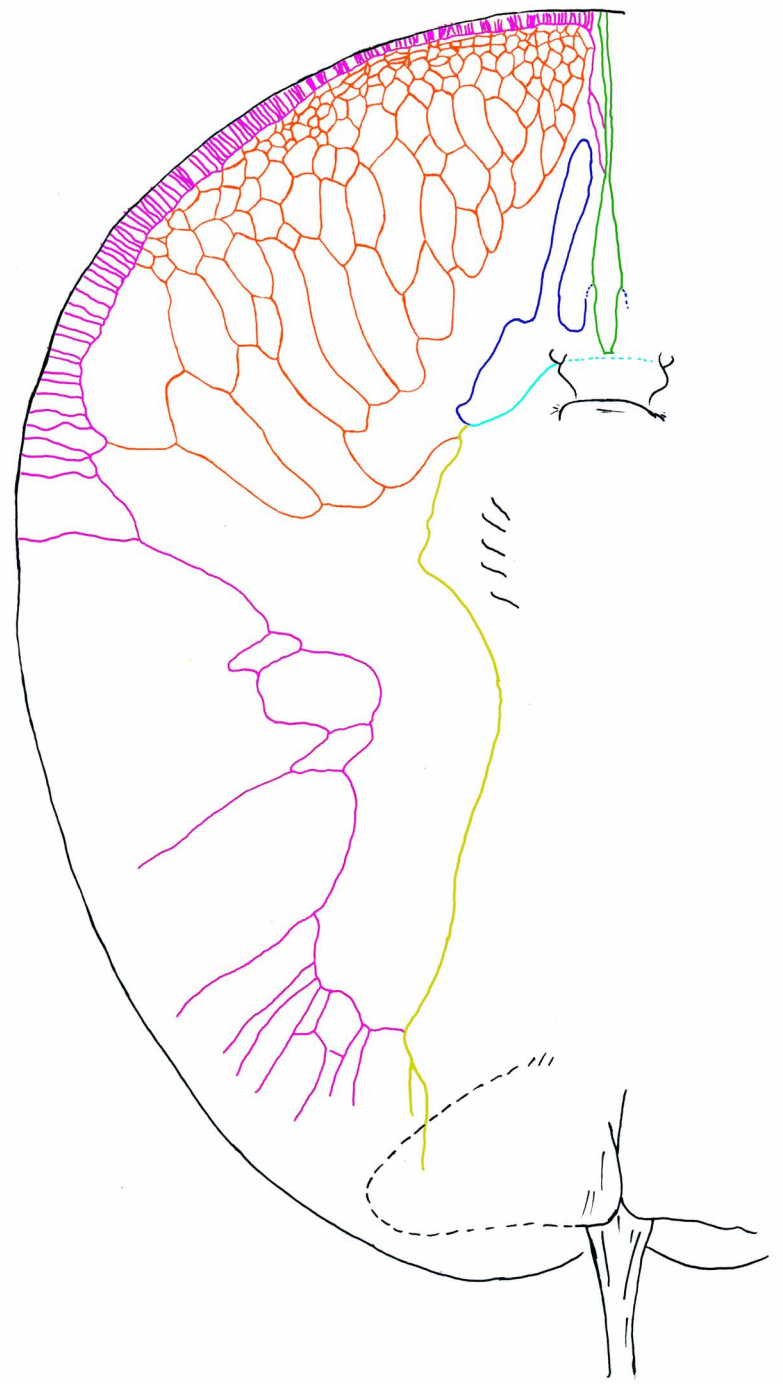

FIGURE 19. Ventral lateral-line canals of a specimen of *Heliotrygon gomesi*, n. sp. (paratype MZUSP 108203). Color scheme is as follows: anterior subpleural tubules, hyomandibular subpleural component (at level of first pair of gill slits) and hyomandibular canal (purple); hyomandibular jugular component (yellow); nasal canal (light blue); prenasal component of nasal canal (green); suborbital component of infraorbital canal (light red); supraorbital canal (dark blue).

Skeletal anatomy. (Figures 20–4). In general, the skeleton of the new genus (based on examinations of both species) is very similar to that of *Paratrygon*. The description below roughly applies to both *H. gomesi* and *H. rosai*, and was based on specimens of both species.

Neurocranium. The neurocranium is relatively elongate, being about as long as the metapterygium, and twice as long as neurocranial greatest width. Neurocranial greatest width at nasal capsule region. Nasal capsules broadly rounded anteriorly and relatively short anteroposteriorly. Postorbital processes wider than preorbital processes. Precerebral and frontoparietal fontenellae elongate, about three-fourths of neurocranial length, and composed of a single structure in adults (no epiphysial bridge present). Precerebral fontanelle extends anteriorly to almost neuro-

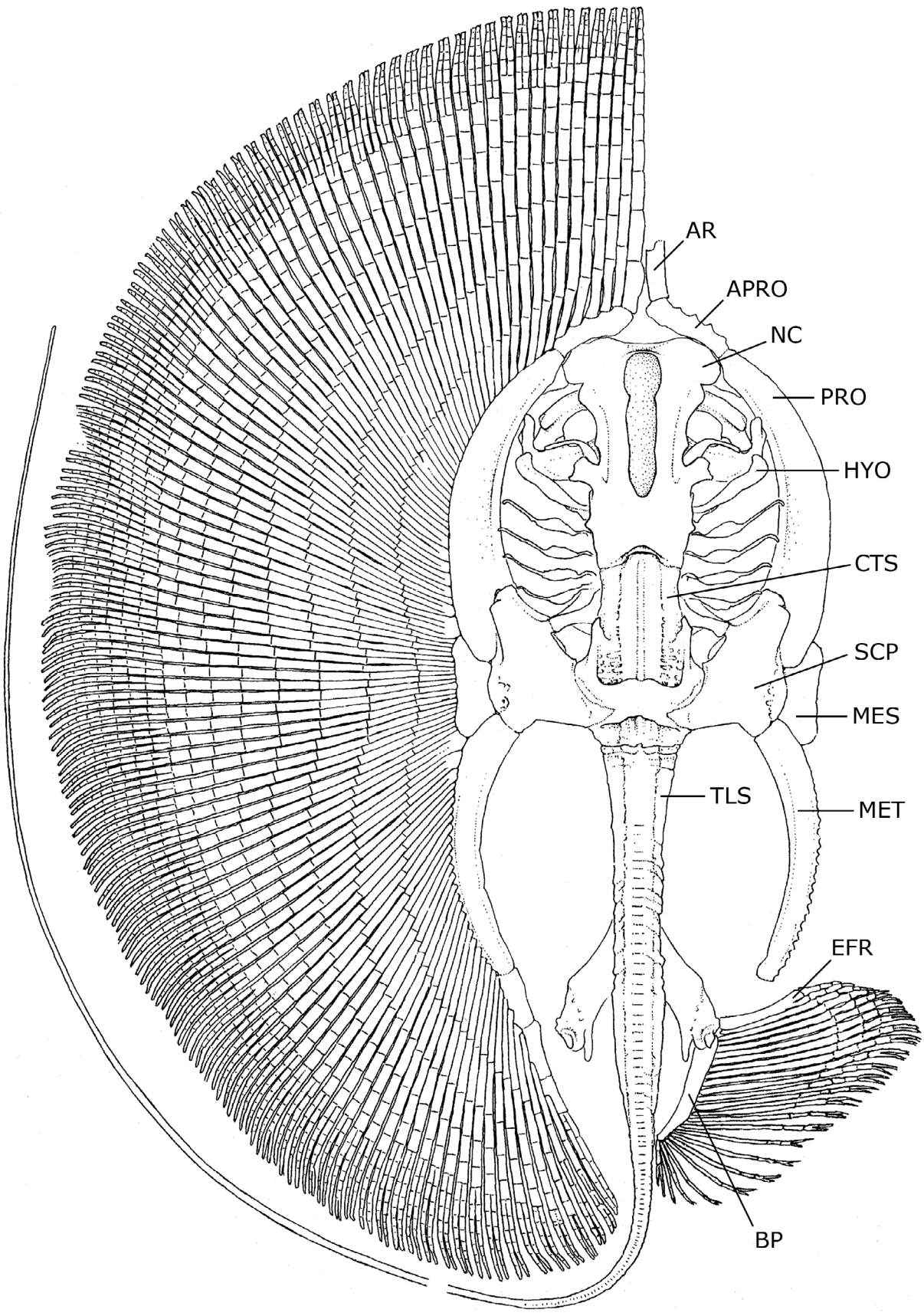

FIGURE 20. Articulated skeleton of *Heliotrygon gomesi*, n. sp. (CU 78486), in dorsoventral view, showing its remarkable morphology. Abbreviations: AR, enlarged anterior pectoral radial element; APRO, anterior segment of propterygium; BP, basipterygium; CTS, cervicothoracic synarcual; EFR, enlarged first pelvic radial element; HYO, hyomandibula; MES, mesopterygium; MET, metapterygium; NC, nasal capsule; PRO, propterygium; SCP, scapular process; TLS, thoracolumbar synarcual.

cranial anterior margin. Post-fontanellae neurocranial length relatively great, about one-third of neurocranial length. Nasal capsules separated by a relatively wide internasal septum, about equal to nasal aperture length. Anterior margin of nasal capsules slightly irregular, with small protuberances medially and at outer corners, articulating with anterior segment of propterygium. No sign of rostral appendix or remnant of rostral process in any specimen. Between pre- and postorbital process, much closer to the postorbital process, is the small, triangular supraorbital process. Preorbital processes small and blunt. Spiracular cartilage (providing support for the anterior spiracular wall) slender and elongate, curved at more or less its midlength. Antorbital cartilage triangular, articulating with posterolateral corner of nasal capsule, and closely associated with propterygium.

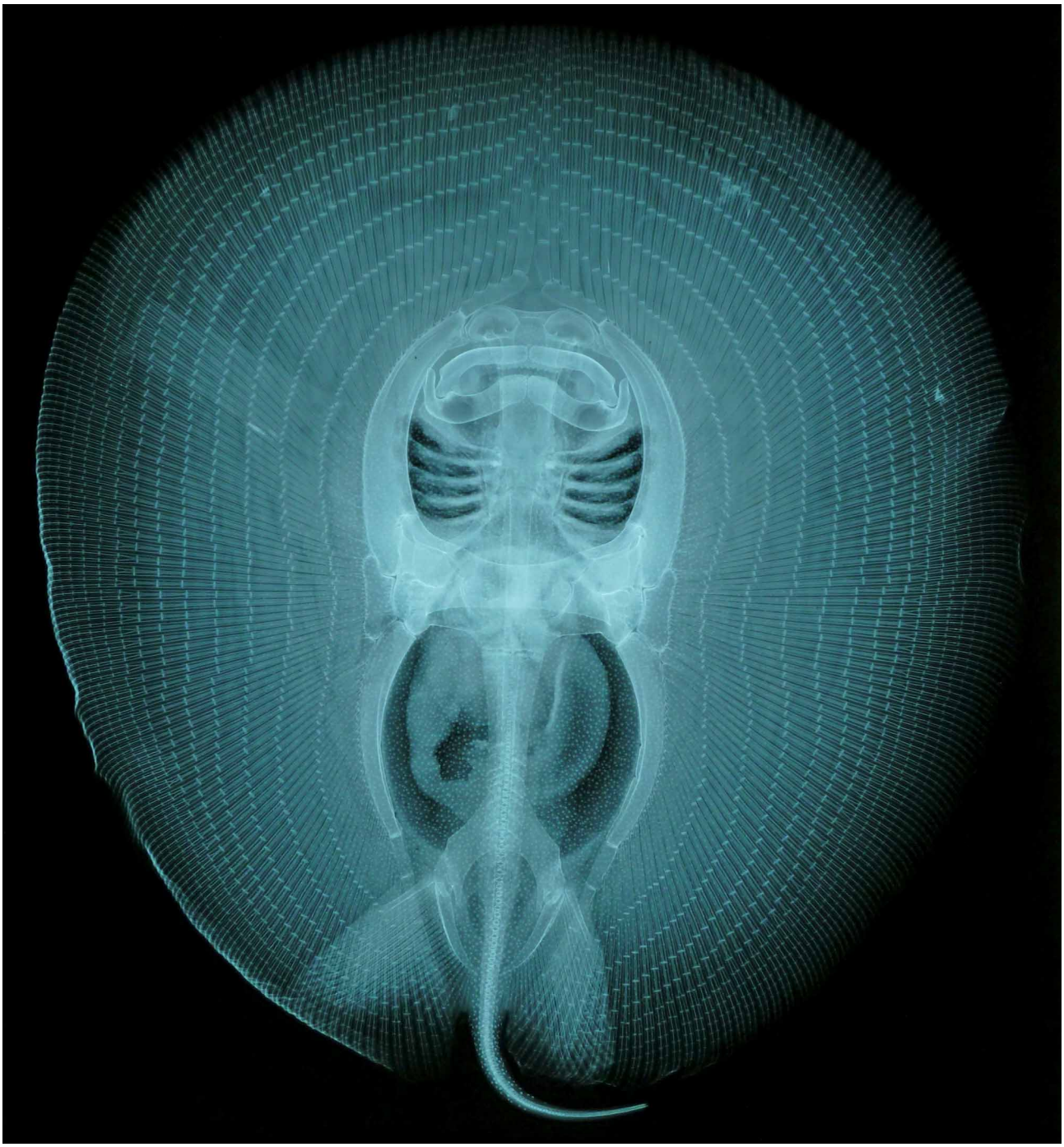

FIGURE 21. Radiograph (CU 78485), in dorsoventral view, depicting morphological aspects of *Heliotrygon gomesi*, n. sp.

Mandibular, hyoid and branchial arches. In general, the mandibular arch resembles that of *Paratrygon*, but slightly less angled and more straight across. Palatoquadrates very slender and relatively straight at anterior mar-

gins. Meckel's cartilages slightly oriented anteriorly at mid-line, but generally also relatively straight. Meckel's cartilages more robust at symphysis, and with well-developed, slender lateral processes. Hyomandibulae more or less straight and relatively short, anteriorly slightly curved toward midline, with small anterior concavity for articulation with Meckel's cartilages. Angular cartilages absent. Basibranchial copula elongate, reaching anteriorly to beyond posterior margin of frontoparietal fontanelle in dorsoventral view, and extending to close to basihyal cartilage. Anterior segment of basibranchial very triangular, acute, and more slender than in other potamotrygonid genera. First hypobranchial elements anteriorly oriented toward midline, extending anteriorly to basibranchial copula extremity. Pseudohyoid arch more slender than succeeding branchial arches. Branchial gill rays reaching propterygium.

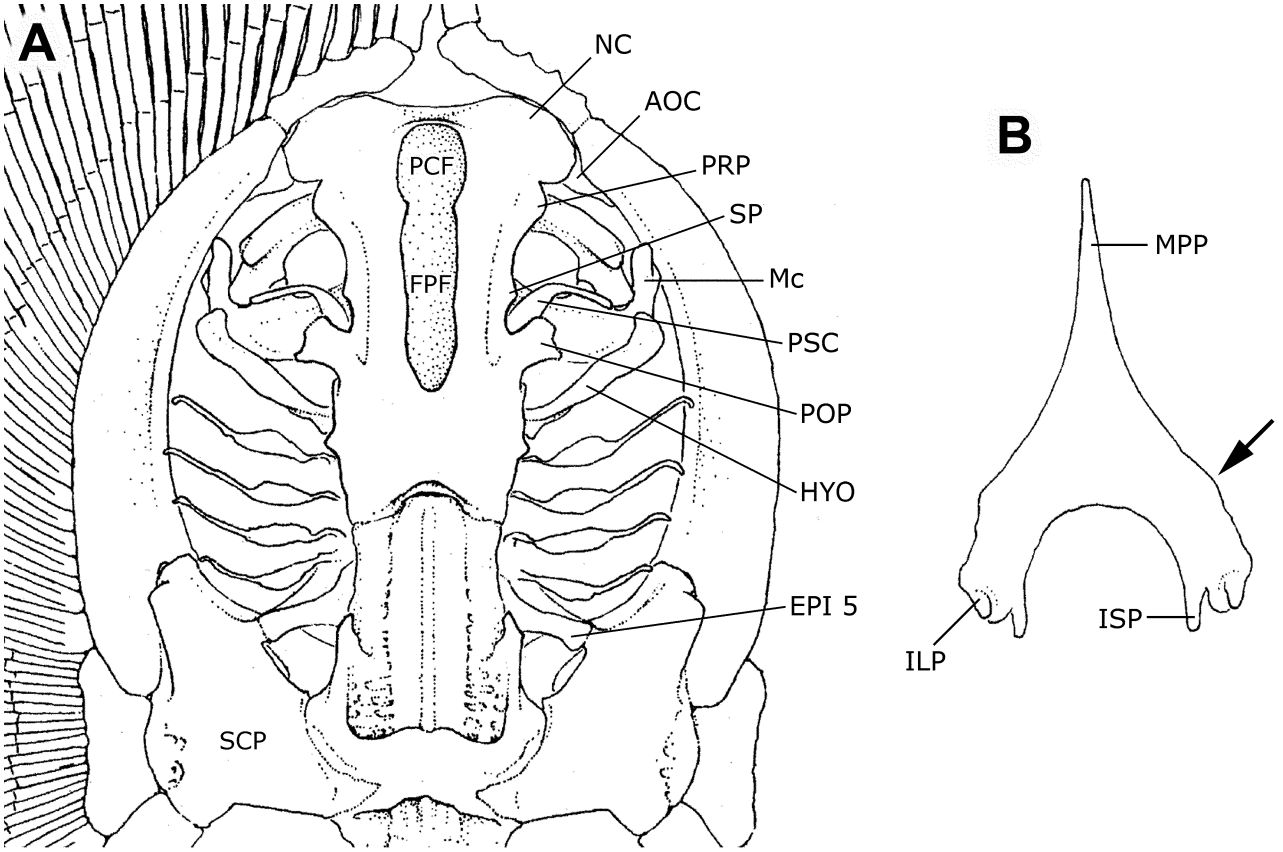

FIGURE 22. Aspects of the splanchnocranium, scapulocoracoid, and pectoral fin skeleton (A), and puboischiadic bar (B) of *Heliotrygon gomesi*, n. sp., in dorsoventral view (based on CU 78456). Abbreviations: AOC, antorbital cartilage; EPI 5, fifth epibranchial element; FPF, frontoparietal fontanelle; HYO, hyomandibula; IP, iliac process; ISP, ischial process; Mc, Meckel's cartilage; MPP, median prepelvic process; NC, nasal capsule; PCF, precerebral fontanelle; POP, postorbital process; PSC, prespiracular cartilage; PRP, preorbital process; SCP, scapular process; SP, supraorbital process. Arrow in (B) depicts very reduced and blunt lateral prepelvic process.

Axial elements. Cervicothoracic synarcual cartilage very robust and elongate, its width anteriorly about equal to posterior neurocranial width, and its greatest width just under greatest width of neurocranium. Lateral stays not projecting laterally to a great extent. Thoracolumbar synarcual strongly calcified laterally and relatively wide, extending from scapulocoracoid to close to puboischiadic bar (posterior to anterior extremity of median prepelvic process). Individual vertebral elements occurring posteriorly beyond level of caudal sting, becoming an uncalcified notochordal extension (cartilaginous rod) well posterior to caudal sting extremity. Transition from mono- to diplospondyly occurs usually slightly caudal to posterior margin of pelvic girdle (usually at between third and fifth centrum posterior to pelvic girdle). Distinct neural elements present even on vertebrae of caudal whip.

Appendicular skeleton. Propterygium relatively stout, widest posteriorly, and anteriorly curved toward midline. Anterior segment of propterygium about one-fourth to one-fifth length of propterygium, closely abutting nasal capsule, and almost contacting its antimere. Mesopterygium also relatively elongate, slightly concave externally,

and more slender anteriorly. Anterior and posterior extensions of mesopterygium rounded. Metapterygium highly arched, more slender than propterygium, articulating posteriorly with three smaller metapterygial segments. Disc with closely articulating pectoral fin radial elements. Radial elements sometimes fused at base, especially those articulating with posterior portion of propterygium and anterior segment of metapterygium. Pectoral radials relatively slender where they articulate with pectoral basals, widening toward middisc, and becoming again more slender distally where they bifurcate. Pectoral radials subdivided into 17 segments (18 in some specimens) from propterygium to outer disc margin; complete subdivision of radials occurs at ninth segment at level of greatest disc width, but at eighth segment closer to anterior disc. Radial subdivision occurs by splitting and strengthening internal calcification in segment medial to segment that is fully subdivided. Radial segments more stout at anteriormost disc on snout region, and becoming progressively shorter toward outer disc margins. Outermost radials with distal subdivided segments closely contacting each other.

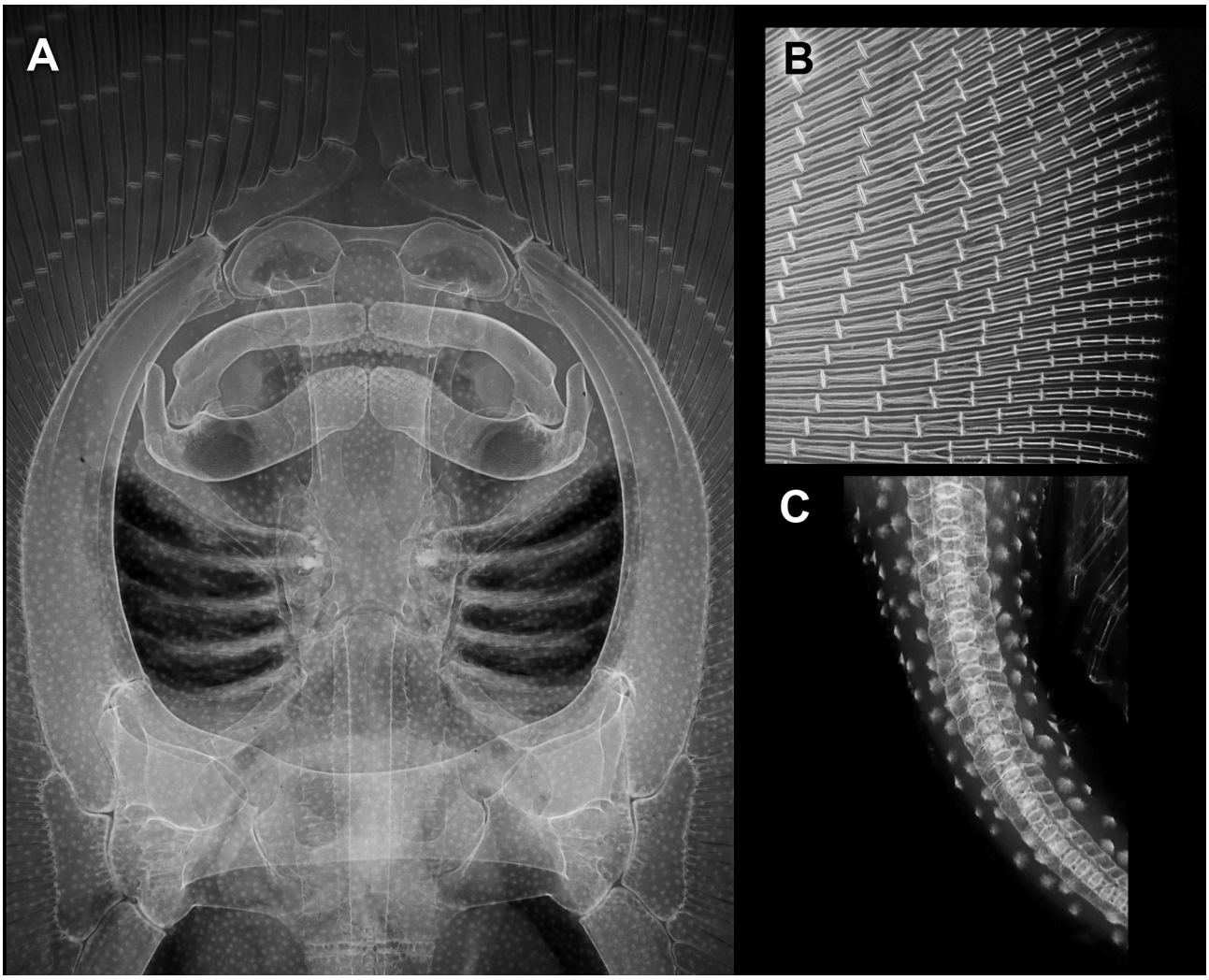

FIGURE 23. Morphological details of *Heliotrygon gomesi*, n. sp., in dorsoventral view (based on CU 78456). A) Splanchnocranium, scapulocoracoid, pectoral basal elements, and anterior disc radials. Notice arrangement of dermal denticles on anteromedial disc region. B) Detail of anterolateral disc region, showing transition to bifurcating radials, usually at 8-9th radial (counting from propterygium). C) Detail of dorsal tail base region showing specific pattern of dermal denticles.

Pelvic girdle very triangular in profile, relatively very stout, with median prepelvic process extending to about anterior one-third of metapterygial length (extent of prepelvic process not visible in radiographs) (Figure 22B). Lateral prepelvic processes reduced to mere rounded corners. Pelvic girdle resembling an inverted "V", with short iliac processes not extending caudally beyond ischial processes. Iliac processes with articular surface for basipterygium and enlarged first pelvic radial element. Ischial processes not very elongate, slender distally. Basipterygium robust, about as wide as posterior portion of metapterygium. Basipterygium curves inward posteriorly, and oriented

obliquely in relation to midline. Pelvic radials subdivided into eight or nine segments, the most proximal much more elongate, extending to about 80% of pelvic fin width; fifth pelvic segment is subdivided.

Clasper skeleton (Figure 24) consists of the following cartilages: two basal segments, a single beta cartilage, axial cartilage, dorsal marginal, ventral marginal, dorsal terminal 2, accessory terminal, and ventral terminal. First basal segment larger and connecting to basipterygium; second basal segment smaller and linked to proximal part of axial cartilage. Beta cartilage originating at first basal segment and distally articulated with dorsal marginal. Axial cartilage straight, depressed anteriorly and distally cylindrical, tapering toward extremity. Ventral marginal long and narrow, with pronounced anterior tip. Two pelvic radials reach anterior tip of ventral marginal (not depicted in illustration, Figure 24). Outer edges of dorsal marginal and dorsal terminal 2 forming the clasper groove externally. Inner edge of posterior portion of dorsal marginal forming dorsal pseudosiphon externally. Dorsal terminal 2 elongated, narrow and oval. Accessory terminal cartilage elongated and fusiform, underlying dorsal terminal 2, and forming ventral pseudosiphon externally from its outer edge. Ventral terminal broad, elongate and oval.

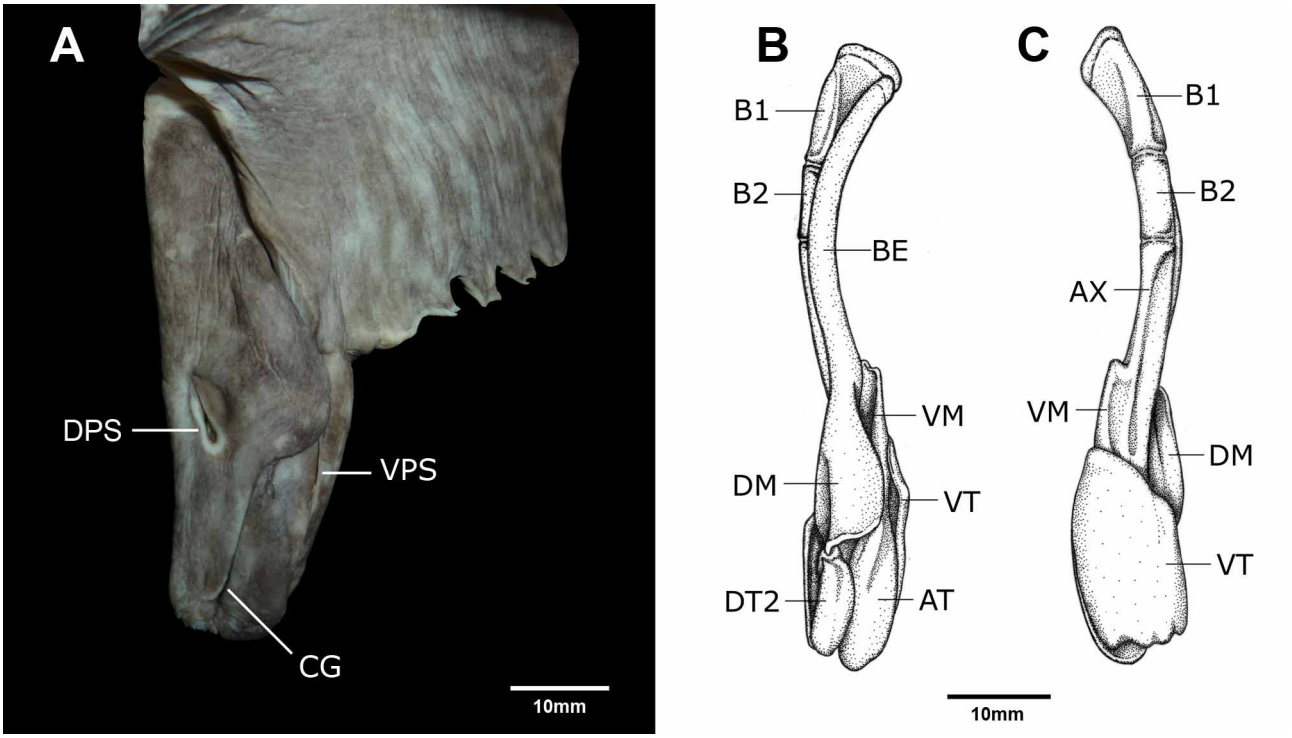

FIGURE 24. Clasper morphology of *Heliotrygon rosai*, n. sp. A) External morphology (holotype, MZUSP 104996). B) Clasper skeleton in dorsal view (MZUSP 108295). C) Clasper skeleton in ventral view (MZUSP 108295). Anterior facing top of page. Abbreviations: AT, accessory terminal cartilage; AX, axial cartilage; BE, beta cartilage; B1, first basal segment; B2, second basal segment; CG, clasper groove; DM, dorsal marginal cartilage; DPS, dorsal pseudosiphon; DT2, dorsal terminal 2 cartilage; VM, ventral marginal cartilage; VPS, ventral pseudosiphon; VT, ventral terminal cartilage.

Cranial, hyoid and mandibular muscles. (Figure 25). A full description of the myology of *Heliotrygon* is being prepared; here we restrict ourselves to features that clarify the affinities of *Heliotrygon* with other potamotrygonids. *Heliotrygon* has a considerably robust mandibular musculature. The short distance between the neurocranium and the branchial region has confined the ventral hyoid muscles to a relatively small area, very similar to the condition in *Paratrygon*. In terms of cranial muscles, *Heliotrygon* has other features in common with *Paratrygon*, hypothesized to be derived: (1) the lateral adductor mandibulae 1 has an elevated number of superficial subdivisions (muscle fibers are internally somewhat mixed); (2) medial portion of spiracularis (spiracularis medialis) is inserted onto Meckel's cartilage, and does not project ventrally as in *Plesiotrygon* and *Potamotrygon*. Spiracularis lateralis muscle inserts onto distal portion of the hyomandibula. Levator palatoquarati muscle wraps around palatoquadrate to insert onto its outer, medial portion. The coracohyoideus muscle shows two muscle fibers oriented in different directions, however an evident division into two separate muscles (as in *Paratrygon* and in some *Potamotrygon* species) is not visible (in *Plesiotrygon*, all the fibers have the same orientation).

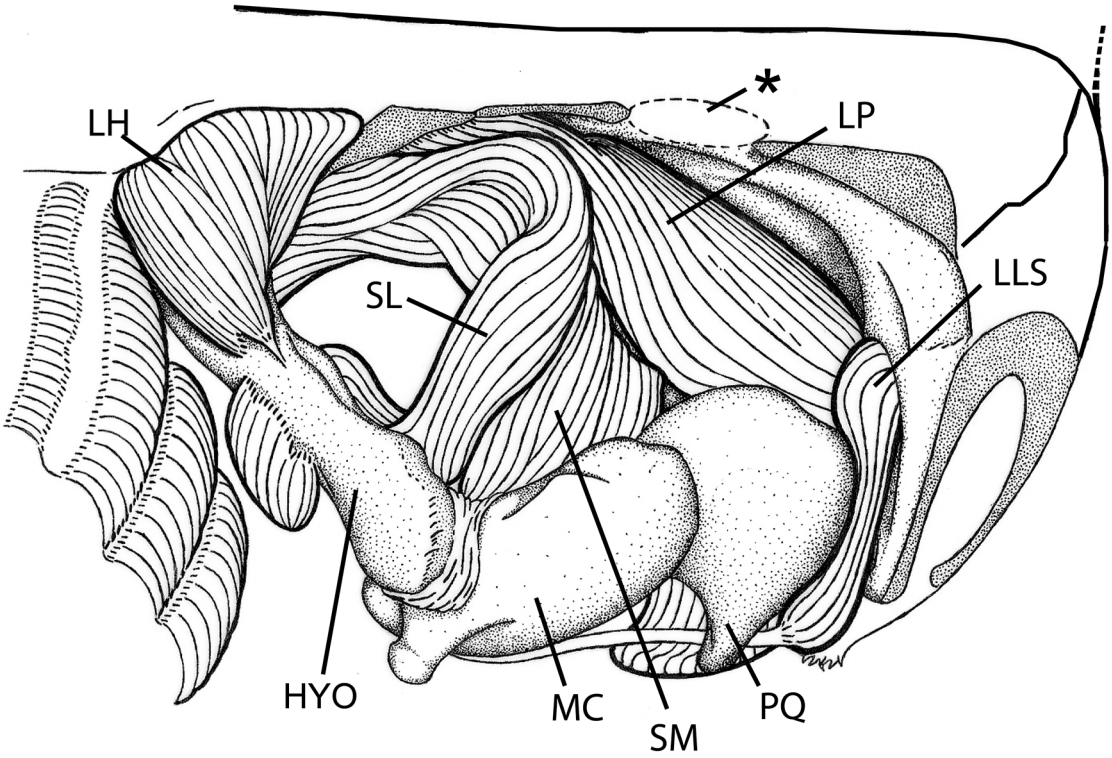

FIGURE 25. Cranial, mandibular, and hyoid muscles of *Heliotrygon rosai*, n. sp. (from MZUSP 108295). Specimen is facing right. Notice that pre- and postorbital processes, nasal capsules, and part of rostral region were cut. Specimen is in dorsolateral view. Abbreviations: HYO, hyomandibula; LH, levator hyomandibularis; LLS, levator labii superioris; LP, levator palatoquadrati; MC, Meckel's cartilage; PQ, palatoquadrate; SM, spiracularis medialis; SL, spiracularis lateralis. Asterisk indicates position of eye.

Phylogenetic relationships of *Heliotrygon*

Heliotrygon shares with *Paratrygon* numerous anatomical features hypothesized to be derived within potamotrygonids, and therefore both genera are best interpreted as sister groups (Figures 26, 27). Some of these features have been mentioned and utilized above in the differential diagnosis of *Heliotrygon*. In addition, both species of *Heliotrygon* clearly share many derived features that corroborate generic monophyly. Further anatomical descriptions and comparisons for some of the myliobatiform taxa below can be found in Lovejoy (1996), McEachran et al. (1996), and Carvalho et al. (2004) (also, see references cited in the latter paper for morphological descriptions of different stingray taxa).

Derived characters of *Heliotrygon*, in addition to the extremely unusual disc proportions (disc highly circular, convex anterior disc and snout region, greatly expanded snout region, disc width and length similar in proportions), include: (1) extreme subdivision of suborbital component of infraorbital canal, forming a complex honeycomb-like pattern anterolaterally on disc; (2) re-orientation toward disc midline of hyomandibular canal (subpleural component) occurring very posterior to level of mouth; (3) subpleural component of hyomandibular canal forming irregular, oval loops lateral and posterior to gill openings; (4) supraorbital loop very slender, extending anteriorly beyond midsnout length; (5) anterior subpleural tubules of hyomandibular canal extremely numerous, much more so than in *Paratrygon*; (6) numerous elongated individual posterior extensions (posterior subpleural tubules), in direction of outer disc margin, of subpleural component of hyomandibular canal; (7) pelvic girdle broadly triangular in shape, resembling an upside-down "V"; (8) pelvic girdle lacking well-defined lateral prepelvic processes; (9) extremely reduced, more or less smooth caudal sting; (10) anterior segment of propterygium abutting anterolateral margins of nasal capsules; (11) basibranchial copula with highly acute anterior extension, reaching anteriorly closer to basihyal; (12) anterior propterygial segments almost contact each other medially, leaving very reduced space anterior to neurocranial rostral region; (13) metapterygium relatively stout and highly arched, reaching laterally to level of propterygium; (14) precerebral fontanelle and frontoparietal fontanelle of about same width, tapering very little posteriorly.

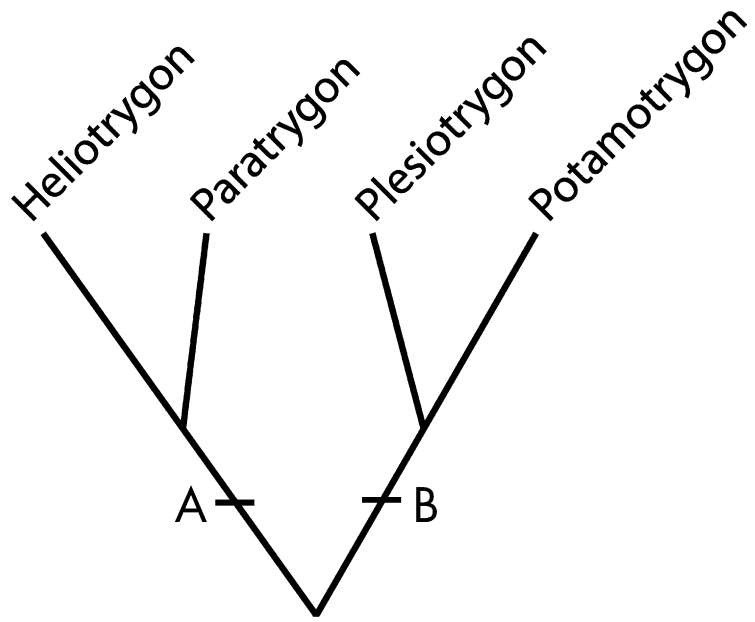

FIGURE 26. Cladogram depicting relationships among genera of Potamotrygonidae, showing sister group relationship between *Heliotrygon* and *Paratrygon*, based on discussion in the text (see Phylogenetic relationships of *Heliotrygon* for characters at indicated nodes and for *Heliotrygon*). For a discussion of myliobatiform phylogeny, see Carvalho et al. (2004) and references cited therein.

Characters hypothesized to be derived for the clade composed of *Heliotrygon* and *Paratrygon* (node A in Figure 26), include the following (plesiomorphic condition in parentheses): (1) supraorbital canal looping anteriorly at more or less level of nostrils (supraorbital canal loops anteriorly clearly lateral to nostrils in *Potamotrygon* and *Plesiotrygon*); (2) suborbital component of infraorbital canal subdivided and highly reticulated on anterolateral ventral disc (not reticulated and relatively simple in *Potamotrygon*, *Plesiotrygon*, dasyatids, urolophids, and urotrygonids; Lovejoy, 1996); (3) very small and blunt preorbital processes, not projecting laterally beyond greatest width of nasal capsules (triangular and relatively larger in *Potamotrygon*, *Plesiotrygon* and other myliobatiforms, even in *Urotrygon*, which has reduced preorbital processes; Carvalho et al., 2004); (4) otico-occipital region of neurocranium elongate, about equal to cranial width at orbital region (otico-occipital region shorter than width at orbital region in *Potamotrygon*, *Plesiotrygon* and other myliobatiforms); (5) internasal septum relatively wide, space between nasal capsules is consequently relatively large (nasal capsules more rounded and very close together in *Potamotrygon* and *Plesiotrygon*); (6) relatively slender palatoquadrate and Meckel's cartilage (these much stouter in *Potamotrygon*, *Plesiotrygon*, dasyatids, urotygonids, urolophids, and more derived myliobatids, but independently derived in gymnurids); (7) extremely stout and anteriorly expanded scapulocoracoid, with anteroposterior expansion slightly greater than one-half of neurocranial length (scapulocoracoid not anteroposteriorly expanded as such in *Potamotrygon*, *Plesiotrygon* and other myliobatiforms; independently derived for gymnurids; Carvalho et al., 2004); (8) mesopterygium articulates with scapulocoracoid through elongated articular surface that is greater in length than mesopterygial width (articular surface with scapulocoracoid curved and short in *Potamotrygon*, *Plesiotrygon* and other myliobatiforms, but independently derived at least in *Dasyatis margarita*; for discussion of this and other characters related to the mesopterygium, see Carvalho et al., 2004); (9) lateral processes of Meckel's cartilage relatively elongate, extending dorsally much more than in *Potamotrygon*, *Plesiotrygon* and more basal myliobatiforms, but independently derived in gymnurids; Carvalho et al., 2004); (10) anteriormost pectoral radials relatively wide and elongated, much more broad than other pectoral radials (pectoral radials more or less of same width in *Potamotrygon*, *Plesiotrygon* and other myliobatiforms, except, perhaps, in *Urotrygon*); (11) elevated number of pectoral radial elements, over 100 (*Plesiotrygon* and *Potamotrygon* with lower total pectoral radials, usually between 75–90; independently derived in *Potamotrygon brachyura* which has on average about 110 pectoral radials); (12) claspers short and stout, barely visible dorsally in adult males at pectoral axil region, and projecting at most to posterior disc level (adult claspers of *Potamotrygon* and *Plesiotrygon* projecting well beyond posterior margin of disc, similar to other myliobatiforms); (13) nostrils very circular and reduced in size (nostrils slit-like, more elongated in *Potamotrygon*, *Plesiotrygon*, dasyatids, urotrygonids, urolophids, and myliobatoids in general, but not in *Hexatrygon* and, to a lesser extent, *Plesiobatis*); (14) beta cartilage of clasper elongated and continuous

with dorsal marginal cartilage (beta cartilage shorter in *Potamotrygon* and *Plesiotrygon*, and generally in myliobatiforms); (15) lateral adductor mandibulae 1 with many superficial subdivisions (not nearly as subdivided in *Potamotrygon*, *Plesiotrygon*, and other benthic myliobatiforms); (16) spiracularis medialis muscle inserts on Meckel's cartilage and does not project ventrally as in *Plesiotrygon* and *Potamotrygon*; (17) antorbital cartilage relatively short and broad, not projecting posteriorly beyond posterior level of preorbital process (antorbital more slender and elongate, projecting at least to posterior level of preorbital process in *Potamotrygon*, *Plesiotrygon* and benthic myliobatiforms in general; independently derived in gymnurids). Some of the characters above (e.g. characters 9, 16) require further comparisons with other myliobatiform taxa in order to better corroborate their placement on our phylogeny.

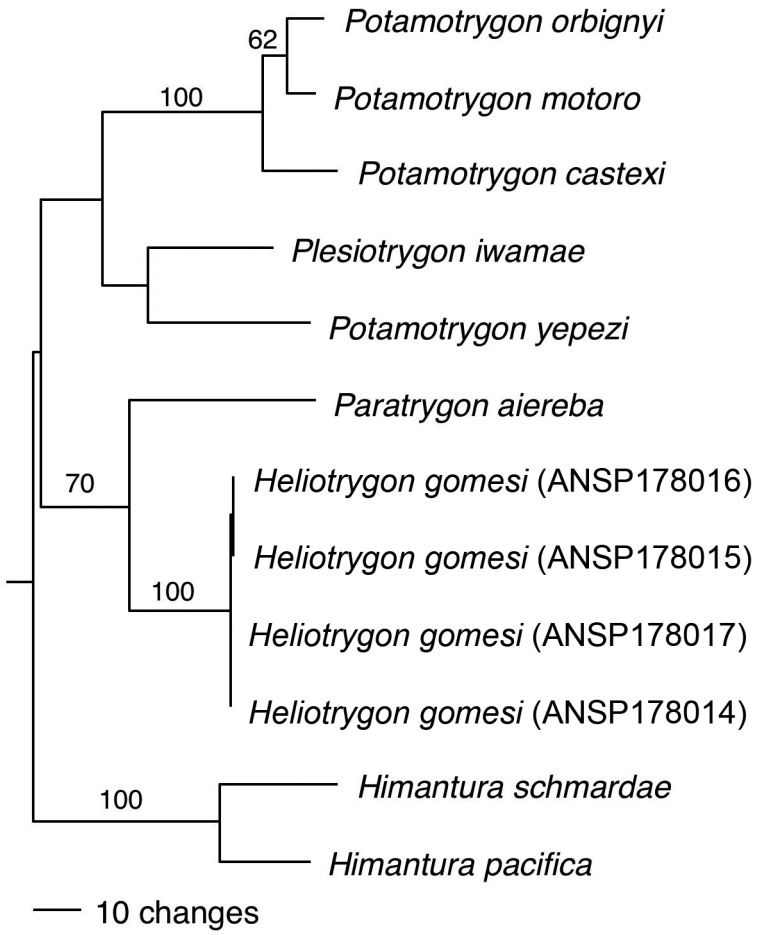

FIGURE 27. Single most parsimonious tree showing phylogenetic relationships among Neotropical freshwater stingray genera based on 637 base pairs of the mitochondrial cytochrome b gene. Numbers above nodes denote bootstrap proportions > 50%; branch lengths proportional to character changes based on DELTRAN optimization; CI = 0.73, RI = 0.75, tree length = 315.

Potamotrygon and *Plesiotrygon* share the following derived features (node B in Figure 26): (1) hyomandibular canal extending posteriorly more medially on anterior ventral disc, re-orienting away from disc margin very anterior to level of mouth (hyomandibular canal positioned ventrally on anterolateral disc margins extending posterolaterally very close to disc margin, and re-orienting medially close to level of nostrils in *Heliotrygon*, *Paratrygon*, dasyatids, urolophids, and urotrygonids, and myliobatoids; Lovejoy, 1996; McEachran et al., 1996); (2) distinct forward loop of suborbital component of the infraorbital canal, positioned lateral to level of nostrils (Lovejoy, 1996); (3) posterior single canal extension of subpleural loop elongated, usually reaching posteriorly to disc margin (extension shorter in *Paratrygon* and *Heliotrygon*, as well as in other myliobatiforms; e.g. Garman, 1888; Chu & Wen, 1979; Lovejoy, 1996); (4) angular cartilages present; a single cartilage in all of our examined material of *Plesiotrygon*, and usually two in *Potamotrygon* (absent in remaining myliobatiforms including *Heliotrygon* and *Paratrygon*; for general discussion on angular cartilages, see Carvalho et al., 2004); (5) strong hyomandibular-

Meckelian ligament (however, this feature may be plesiomorphic at this level; this character was extensively discussed in Carvalho et al., 2004).

We also undertook a molecular phylogenetic analysis. Our sequencing of cytochrome *b* from *Heliotrygon gomesi* yielded four sequences that were 637 base pairs in length, and have been deposited in Genbank (numbers JF358007-JF358010). Two haplotypes were detected, differing by a single base position, with each haplotype occurring in two of the sequenced individuals. We combined our new sequences in a matrix with the published sequences from Lovejoy et al. (1998) that include the three previously known Neotropical freshwater stingray genera (*Potamotrygon*, *Plesiotrygon*, and *Paratrygon*), as well as *Himantura schmardae* and *H. pacifica*. Uncorrected pairwise sequence divergence between *Heliotrygon* and the other genera is 14.2–14.6% (*Himantura*), 10.3–11.5% (*Potamotrygon*), 9.9–10.1% (*Plesiotrygon*), and 8.5–8.7% (*Paratrygon*). Phylogenetic analysis produced a single most parsimonious tree of 315 steps (Figure 27). This tree supports the position of *Heliotrygon* and *Paratrygon* as sister taxa, with a bootstrap proportion of 70%. These taxa are the sister group to a clade composed of *Plesiotrygon* and *Potamotrygon* species. Thus, molecular data from the cytochrome *b* gene are largely in agreement with the morphological analysis presented here.

Acknowledgements

Members of the Laboratório de Ictiologia da Universidade de São Paulo, namely João Paulo Capretz, João Pedro Fontenelle, Diego Vaz, André Casas, Mateus Soares, and Maíra Portella are acknowledged for their support and substantive technical assistance during the final phases of this project. A special acknowledgement is owed to Murilo Carvalho for his dedication in helping to bring this project to fruition. MRC is grateful to Flávio A. Bockmann (Departamento de Biologia, FFCLRP, USP) and Ulisses L. Gomes (Universidade do Estado do Rio de Janeiro) for their intellectual support and discussions over the years. José Lima de Figueiredo, Naércio A. Menezes, and Osvaldo T. Oyakawa (MZUSP) are thanked for their support during numerous visits to the MZUSP. Melanie Stiassny, Scott Schaefer, John Sparks, Robert Schelly, Rad Arindell and Barbara Brown (AMNH) are thanked for their hospitality during visits. For obtaining specimens and other help with collection work, we thank Mark Sabaj (ANSP), Mike Littman and Linder Isuiza. Hernan Ortega is thanked for facilitating field work in Peru. Dave Taylor assisted NRL with measurements. Illustrations of whole specimens and of the skeleton were rendered by Ian Hart (New York), and those of the clasper and ventral lateral-line by Wilson S. Júnior (São Paulo). Gilmar de Oliveira (Radiologia, Hospital Central, USP, Ribeirão Preto), Robert Schelly (AMNH), Dave Catania (Los Angeles County Museum), Graham Crawshaw and Michelle Lovering (Toronto Zoo), and Hugo Hidalgo (Faculdade de Medicina Veterinária e Zootecnia, USP, São Paulo), are sincerely thanked for taking radiographs of specimens. For providing material crucial for this paper, we are grateful to Fernando P. L. Marques (whose field work is supported by Fapesp grants 03/01816-2, 05/01299-3, 08/09436-8), Mauro C. Júnior and Marcus V. Domingues (Departamento de Zoologia, Instituto de Biociências, Universidade de São Paulo, São Paulo), as well as Richard Ross. P. C.-Almeida generously provided the specimen (along with the damaged specimen) that eventually became the holotype of *Heliotrygon rosai*, for which she is gratefully acknowledged. This project was funded by the Fundação de Amparo à Pesquisa do Estado de São Paulo (FAPESP) through grants to the first author (02/06459-0, 10/51193-5), along with financial support from the Conselho Nacional de Desenvolvimento Científico e Tecnológico (CNPq 303061/2008-1). Financial support for NRL was provided by an NSERC Discovery Grant.

References

Araújo, M.L.G. (1998) Biologia reprodutiva e pesca de *Potamotrygon* sp. C (Chondrichthyes, Potamotrygonidae) no médio rio Negro, Amazonas. Unpubl. Master's diss., Instituto Nacional de Pesquisas da Amazônia, Universidade do Amazonas.

Bigelow, H.B. & Schroeder, W.C. (1953) The Fishes of the Western North Atlantic, Part II: Sawfishes, Skates, Rays and Chimaeroids. *Memoirs Sears Foundation for Marine Research*, (2), 1–588.

Carvalho, M.R. de, Lovejoy, N.R. & Rosa, R.S. (2003) Family Potamotrygonidae. Pp. 22–29. *In:* Reis, R.E, Ferraris Jr, C.J. & Kullander, S.O. (Eds.). *Checklist of the Freshwater Fishes of South and Central America*. Porto Alegre, EDIPUCRS, 729 pp.

Carvalho, M.R. de, Maisey, J.G. & Grande, L. (2004) Freshwater stingrays of the Green River Formation of Wyoming (Early Eocene), with the description of a new genus and species and an analysis of its phylogenetic relationships (Chondrich-

thyes: Myliobatiformes). *Bulletin of the American Museum of Natural History*, 284, 1–136.
Castex, M.N. (1963) *La raya fluvial. Notas histórico-geográficas.* Librería y Editorial Castellví, Santa Fe. 120 pp.
Chu, Y.T. & Wen, C.M. (1979) A study of the lateral-line canals system and that of Lorenzini ampullae and tubules of Elasmobranchiate fishes of China. Monograph of Fishes of China. 2. Shangai, People´s Republic of China: Shangai Science and Technology Press.
Compagno, L.J.V. (2005) Checklist of living Chondrichthyes. Pp. 503–548. *In:* Hamlett, W. C. (ed.), *Reproductive Biology and Phylogeny of Chondrichthyes, Sharks, Batoids and Chimaeras.* Science Publishers, Inc. Enfield (NH), USA.
Compagno, L.J.V. & Roberts, T. (1982) Freshwater stingrays (Dasyatidae) of southeast Asia and New Guinea, with description of a new species of Himantura and reports of unidentified species. *Environmental Biology of Fishes*, 7(4), 321–339.
Deynat, P. & Séret, B. (1996) Le revêntement cutané des raies (Chondrichthyes, Elasmobranchii, Batoidea) I – Morphologie et arrangement des denticules cutanés. *Annales des Sciences Naturelles, Zoologie* 17 (2), 65–83.
Deynat, P. (2006) *Potamotrygon marinae* n. sp., une nouvelle espèce de raies d'eau douce de Guyane (Myliobatiformes, Potamotrygonidae) *Comptes Rendu Biologies*, 329 (7), 483–493.
Dingerkus, G. & Uhler, L.D. (1977) Enzyme clearing of alcian blue stained whole smalle vertebrates for demonstration of cartilage. *Stain Technology*, 52(4), 229–232.
Ewart, J.C. & Mitchell, H.C. (1892) On the lateral sense organs of elasmobranchs. II. The sensory canals of the common skate (*Raja batis)*. *Transactions of the Royal Society of Edinburgh*, 37, 87–105.
Garman, S. (1877) On the pelvis and external sexual organs of selachiens, with special reference to the new genera *Potamotrygon* and *Disceus*. *Proceedings of the Boston Society of Natural History,* 19, 197–215.
Garman, S. (1888) On the lateral canal system of the Selachia and Holocephala. *Bulletin of the Museum of Comparative Zoology*, 17, 57–119.
Garman, S. (1913) The Plagiostomia (sharks, skates and rays). *Memoirs of the Museum of Comparative Zoology* 36, 515p., 77 plates.
Hubbs, C.L. & Ishiyama, R. (1968) Methods for the taxonomic study and description of skates (Rajidae). *Copeia*, 1968 (3), 483–491.
Ishihara, H. & Taniuchi, T. (1990) A strange potamotrygonid ray (Chondrichthyes: Potamotrygonidae) from the Orinoco river system. Pp. 91–97. *In*: Oetinger, M. I. & Zorzi, G. D (Eds.), *The Biology of Freshwater Elasmobranchs, a symposium to honor Thomas B. Thorson*. *Journal of Aquariculture and Aquatic Sciences*, 7, 162 p.
Last, P.R. & Compagno, L.J.V. (1999) Dasyatididae. Stingrays. Pp. 1479–1505. *In*: Carpenter, K.E. & Niem, V.H. (Eds.) FAO species identification guide for fishery purposes. *The living marine resources of the Western Central Pacific*. Vol. 3. Batoid fishes, chimaeras and bony fishes part 1 (Elopidae to Linophrynidae). FAO, Rome.
Last, P.R. & Stevens, J.D. (2009) *Sharks and rays of Australia*. 2nd Edition. Cambridge, Mass.: Harvard University Press; 644 p.
Lovejoy, N.R. (1996) Systematics of myliobatoid elasmobranchs: with emphasis on the phylogeny and historical biogeography of neotropical freshwater stingrays (Potamotrygonidae: Rajiformes). *Zoological Journal of the Linnaean Society*, 117, 207–257.
Lovejoy, N.R., Birminghan, E. & Martin, A.P. (1998) South American rays came in with the sea. *Nature*, 396, 42–422.
McEachran, J.D., Dunn, K.A. & Miyake, T. (1996) Interrelationships within the batoid fishes (Chondrichthyes, Batoidea). Pp. 63–84. *In:* Stiassny, M.L.J.; Parenti, L.R. & Johnson, G.D. (eds.). *Interrelationships of Fishes*. Academic Press, New York.
Miyake, T., McEachran, J.D & Hall, B.K. (1988) Edgeworth's legacy of cranial muscle development with an analysis of muscles in the ventral gill arch region of batoid fishes (Chondrichthyes: Batoidea). *Journal of Morphology*, 212, 213–256.
Müller, J. & Henle, F.G.J. (1841) *Systematische beschreibung der Plagiostomen.* Verlag von Veit, Berlin.
Nishida, K. (1990) Phylogeny of the suborder Myliobatidoidei. *Memoirs of the Faculty of Fisheries Hokkaido University* 37 (1/2), 1–108.
Rosa, R.S. (1985a) A systematic revision of the South American freshwater stingrays (Chondricthyes: Potamotrygonidae). Unpublished PhD diss., College of William and Mary, Williamsburg, xvi + 523p.
Rosa, R.S. (1985b). Further comment on the nomenclature of the freshwater stingray *Elipesurus spinicauda* Schomburgk, 1843 (Chondrychthyes, Potamotrygonidae). *Revista Brasileira de Zoologia*, 3(1), 27–31.
Rosa, R.S. (1990) *Paratrygon aiereba* (Muller & Henle, 1841): the senior synonym of the freshwater stingray *Disceus thayeri* Garman, 1913 (Chondrychthyes: Potamotrygonidae). *Revista Brasileira de Zoologia* 7(4), 425–437.
Rosa, R.S., Castello, H.P. & Thorson, T.B. (1987) *Plesiotrygon iwamae*, a New Genus and Species of Neotropical Freshwater Stingray (Chondrychthyes: Potamotrygonidae). *Copeia*, 1987 (2), 447–458.
Rosa, R.S., Carvalho, M. R. de & Wanderley, C.A. (2008) *Potamotrygon boesemani* (Chondrichthyes: Myliobatiformes: Potamotrygonidae), a new species of Neotropical freshwater stingray from Surinam. *Neotropical Ichthyology*, 6 (1), 1–8.
Rosa, R.S., Charvet-Almeida, P. & Quijada, C.C.D. (2010) Biology of the South American potamotrygonid stingrays. Pp. 241–281. *In:* Carrier, J.C.; Musick, J.A. & Heithaus, M.R. (Eds.), *Sharks and Their Relatives Ii: Biodiversity, Adaptative Physiology, and Conservation*. CRC Press, Florida.
Ross, R.A. & Schäfer, F. (2000) *Aqualog Süsswasser Rochen: Freshwater Rays.* Verlag ACS, Mörfelden-Walldorf.
Silva, J.P.C.B. da & Carvalho, M.R. de (in press) A taxonomic and morphological redescription of *Potamotrygon falkneri* Castex & Maciel, 1963 (Chondrichthyes: Myliobatiformes: Potamotrygonidae). *Neotropical Ichthyology*, 2011.
Swofford, D.L. (2002) PAUP*. *Phylogenetic Analysis Using Parsimony (*and Other Methods).* Version 4.0b10. Sinauer Associates, Sunderland, MA.
Taniuchi, T. & Ishihara, H. (1990) Anatomical comparison of claspers of freswater stingrays (Dasyatidae and Potamotrygonidae). *Japanese Journal of Ichthyology*, 37 (1), 10–16.
Thorson, T.B., Brooks, D.R. & Mayes, M.A. (1983) The evolution of freshwater adaptation in stingrays. *National Geographic Society Research Reports*, 15, 663–694.